LTV Missiles and Electronics Group
Missiles Division

Final Report
Contract N00014-87-C-0114

A Nonlinear-Optical Method for Combining High Power Laser Beams in Gases or Plasmas

31 May 1988

(4)

LTV Missiles and Electronics Group
Missiles Division
Report No. 3-45400/8R-66

Final Report
Contract N00014-87-C-0114

A Nonlinear-Optical Method for Combining High Power Laser Beams in Gases or Plasmas

31 May 1988

Jay S. Chivian, C. D. Cantrell, III, C. A. Glosson,
W. D. Cotten, S. F. DiMarco, and S. T. Garner

Prepared for:

Office of Naval Research
800 North Quincy Street, BCT #1
Arlington, VA 22217-5000
Attn: Lt. Kenneth P. Morton, Code 111D

Prepared by:

LTV Missiles and Electronics Group
LTV Missiles Division
P. O. Box 650003
Dallas, TX 75265-0003

Supported by:

Center for Applied Optics
University of Texas at Dallas
P. O. Box 830688
Richardson, TX 75083-0688

TABLE OF CONTENTS

1.0 INTRODUCTION

1.1 Objective

The purpose of the effort discussed in this report was to investigate concepts for laser-controlled optics via near-resonance nonlinear dispersion, so that a laser-induced index grating which is capable of high power laser beam combining might be produced and demonstrated.

1.2 Background

The principle of coherent addition of several input laser beams into one output beam had been demonstrated by the use of binary phase gratings.[1] Properly shaped phase gratings had been etched onto a solid surface, establishing that multiple laser beams can be combined into a single beam with good conversion efficiency.

For high power beams, the limited damage thresholds and maximum permissible thermal loading of solid state devices encouraged a search for more satisfactory working media. Gases and plasmas appeared to offer better solutions as working media. It had been predicted that two laser fields of differing wavelengths interacting with a collision-dominated atomic or molecular system with three effective energy levels could influence one another in a nonreciprocal manner; the creation of and interaction with a grating via near-resonance nonlinear dispersion thus should provide a method for low power laser beams to create a grating in which other beams combined to form a high power beam.[2,3]

With these basic concepts in mind, we proposed to investigate the feasibility of using overlapping laser beams to write a grating or thick hologram in the index of refraction of a gas or plasma with a weak beam under such conditions that the grating would not be destroyed by the beams the grating was designed to deflect; to find media in which this could be accomplished for laser wavelengths of interest; and to undertake proof-of-principle and exploratory experiments on promising systems.

The key technical issues which were addressed can be expressed as two simple questions: (1) can a grating appropriate for beam combining be made in a gaseous medium, and (2) can high power beams really be controlled by lower power beams using near-resonance nonlinear dispersion?

This report reviews the results of the technical effort expended from 28 December 1986 to 31 March 1988. The report is organized so that the results of the proposed tasks are presented each in its own subsection under 2.0 - Technical Discussion and Results. Section 3.0 is a summary and Section 4.0 makes recommendations for future work.

2.0 TECHNICAL DISCUSSION AND RESULTS

2.1 Task 1 - Identification of candidate media for beam combining

Preliminary investigations were undertaken in search of a candidate which would be appropriate for successful proof-of-principle demonstrations. The requirements placed on the candidate material were that it have a three level configuration with dipole-allowed transitions near available laser frequencies, and that there exist a sufficient amount of technical information detailing specific spectroscopic data and anharmonicity constants. A survey of the literature revealed one promising candidate almost immediately: sulfur hexafluoride (SF_6). It was decided that this medium was suitable for purposes of proof-of-principle experiments; it was selected with the idea that the literature would continue to be examined for other candidates which might prove to be better materials for scale-up. Appropriate constants and spectroscopic data pertinent to SF_6 were obtained from the literature for use in a computer code designed to calculate near-resonance nonlinear dispersion relations.

The reasons for choosing SF_6 were as follows: first, the properties of SF_6 are reasonably well known and there is a large body of scientific literature to support most work done with this material. Furthermore, the frequencies of the two dipole-allowed transitions of SF_6, the ν_4 and ν_3 modes, have frequencies of $615cm^{-1}$ and $948cm^{-1}$ respectively, which are near lines from CF_4 and CO_2 lasers. In the SF_6 three level system, the CO_2 laser is used as the probe or high power laser and the CF_4 is used as the pump or control laser. Both of these laser sources are readily available or can be made easily, so calculations based on their spectroscopic properties could begin at once using SF_6 as the nonlinear material.

Investigations have shown at least two other promising materials: 1,1,1-trifluoroethane (Figure 2.1.1) with frequencies at $967cm^{-1}$ for the CH_3 rocking and $3035cm^{-1}$ for the CH stretching bond which overlaps the P(13) and P(18) lines from an HF laser, and methyl fluoride (Figure 2.1.2) with frequencies at $1048cm^{-1}$ for the CF stretching bond lying within the 9.4cm sideband of CO_2 and $2916cm^{-1}$ and 2998^{-1} for the CH stretching bond which may have an overlap with an N_2 or HF laser. Both of these materials were discarded for the initial tests

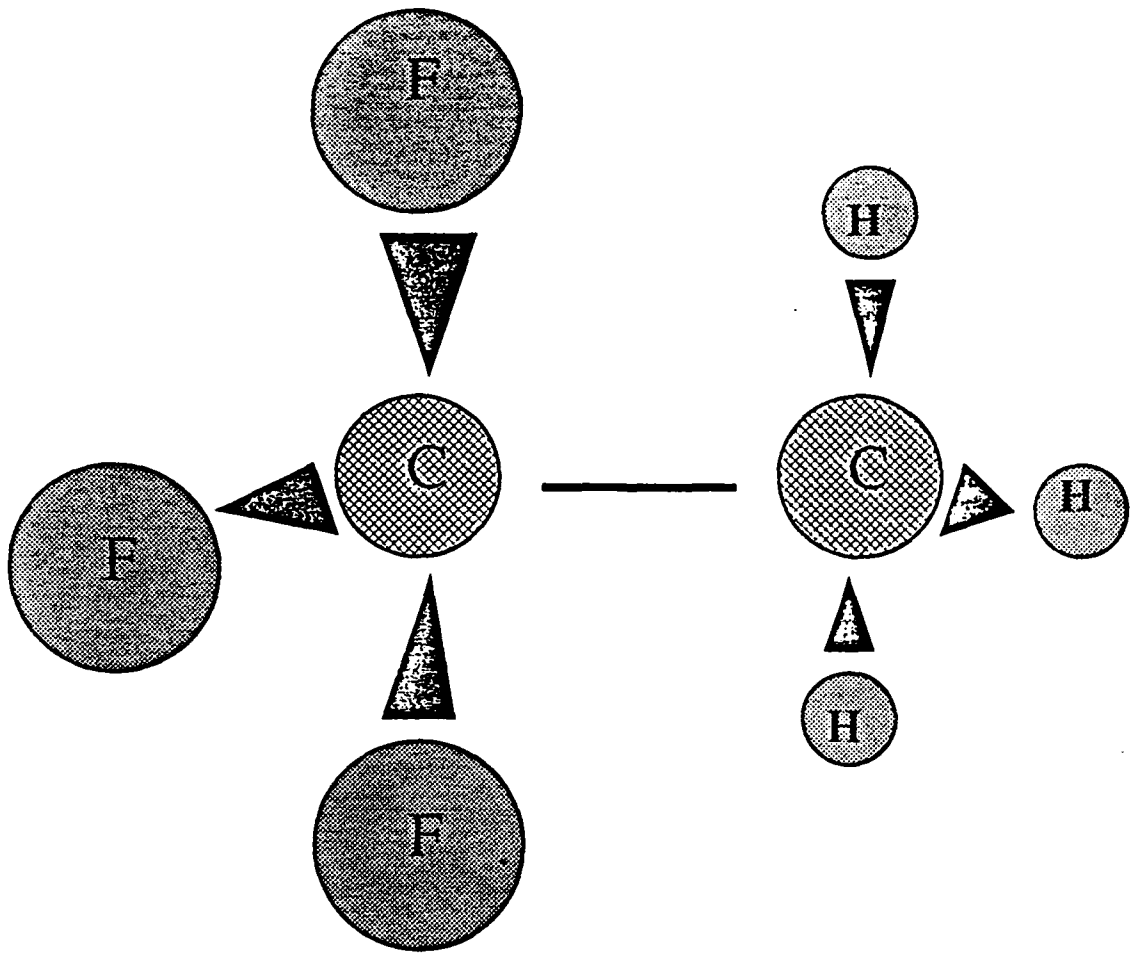

1,1,1-trifluoroethane

Permanent dipole moment = 2.27 +/- .04 D

Relavent Spectral Bands		Laser Overlap Bands
3035 cm^{-1}	C-H stretching	HF laser P(13) line 3031.10 cm^{-1} HF laser P(18) line 3037.70 cm^{-1}
967 cm^{-1}	CH_3 rocking	CO_2 laser

Figure 2.1.1 Candidate medium H_3CCF_3

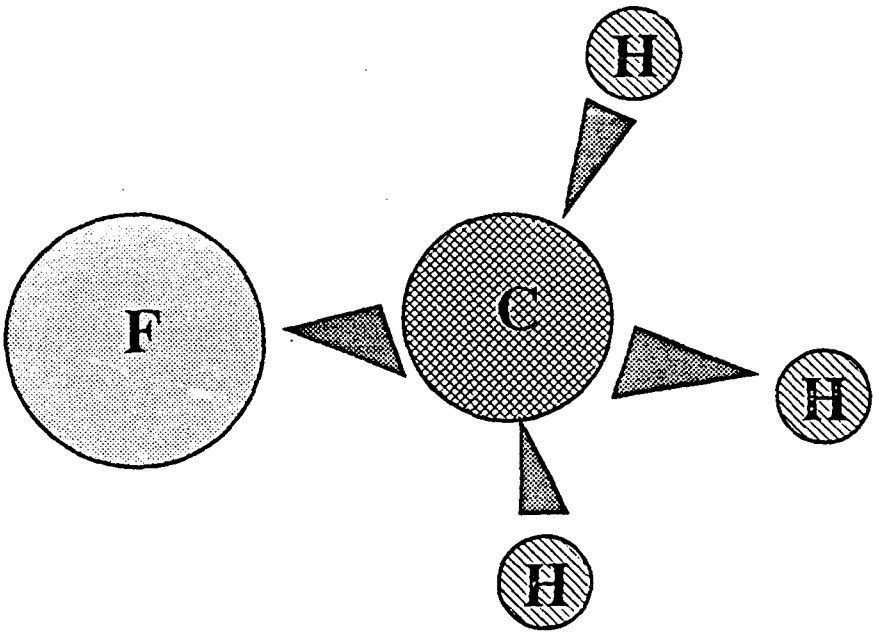

Methyl Fluoride

Permanent dipole moment = 1.855 +/- .0015 D

Relavent Spectral Bands		Laser Overlap Bands
1048.6100 cm^{-1}	C - F stretching	CO_2 laser 9.4 cm side band
2916 cm^{-1}	C - H stretching	Possible N_2 laser or HF laser bands
2998 cm^{-1}	C - H stretching	

Figure 2.1.2 Candidate medium CH_3F

because of their toxicity for which extra precautions and safety devices would have been needed in the lab. In contrast, SF_6 is stable and unreactive, and although it is an asphyxiant, a simple ventilation system is adequate for safe operation.

An existing code evaluated dispersion relations for a three level system, including the effects of saturation by the pump radiation field, when either the probing or pumping field was increased in strength or shifted in frequency. A slight modification of this code was necessary in order to examine the effects of a spatially varying incident radiation field. Essentially, the code solved the steady state density matrix equation for each grid point, with different grid points having different strengths of the pumping field. The result was a profile of the index of refraction as seen by the probe radiation field. With this tool and proper spectroscopic data obtained from the literature, it was possible for an experiment to be designed for the project.

2.2 Task 2 - Determination of the grating profile

In October 1986, in anticipation of beginning this project, LTV acquired a copy of the computer programs known as the Omega codes.[4] These programs were written for use on a CTSS Cray, but will function in a satisfactory manner on a VAX 11/780 or 8650 with only minor modifications dealing with input and output statements.

The main program calculates the diffracted orders, the angle of diffraction, the efficiency of the orders, and the sum of the efficiencies for gratings having finite or infinite conductivity, arbitrary groove shape, covered or not by an arbitrary number of dielectric layers. TE or TM polarization may be treated by the program. The material interfaces may be plane or modulated; if the latter, the modulated interfaces may interpenetrate. The program restricts the ratio of wavelength to groove spacing to $\lambda/d \geq 0.2$ for all cases. The auxiliary programs (1) generate input files for the main program, (2) calculate Fourier coefficients for any grating profile consisting of connecting straight lines, and (3) provide input for a plotting routine to graph diffraction efficiency vs angle of incidence for the order range -3 to +3.

These programs, although sophisticated and powerful, were not suitable for our application because they do not readily adapt to the case of a grating which consists only of an index variation in the planes parallel to the grating surfaces. Consequently we elected not to pursue modification of these codes which were developed for other purposes, but to develop our own formalism for direct application to our specific problems.

Therefore, work began on codes to examine the effects of diffraction gratings on coherent radiation fields. Much work had already been done on coupled wave theory for thick transmission gratings, which we used as the basis for our work. The grating formalism here relies heavily on that developed by Gaylord and coworkers.[5-9] The code to examine this formalism in context of our problem was the first significant portion of Task 2. From the formalism previously developed, it was necessary to include the effects of absorption and polarization of the incident field into a single comprehensive code. At present the code remains in two independent parts, one for each of the orthogonal incident linear polarizations, E-mode and H-mode.

With this simple model representing the effect of a diffraction grating on the radiation field present in our problem, it was possible to begin the conceptual design phase of the project. It became quite clear that a simple grating configuration would contribute to the successful operation of the proof-of-principle experiments. A simple grating would be relatively insensitive to the thickness of the grating, moderately insensitive to the relative intensities of the pump and probe fields, and insensitive to other complicating factors such as gaussian beam profiles, self-diffraction, and laser beam depletion effects. After preliminary investigations to familiarize us to the workings of the code, a grating profile which would combine two probe beams was selected. In addition, combining only two beams requires a reasonably simple experimental apparatus which allows a single beam to be split by a beam splitter and subsequently recombined by the diffraction grating with only the absorption losses inherent to SF_6. Since the thick grating, or holographic, regime is being employed, there exists an extreme phase sensitivity of the output field to the incident phases and incident angles of the laser beams to be combined. To minimize the effect of this phase sensitivity, which becomes more delicate with an increasing number of incident fields, it was necessary to devise the simplest

grating possible, that which combined only two laser beams. Furthermore, since the most efficient gratings were ones in which the profile followed some previously explored and well-defined curves such as a sinusoidal curve, and since SF_6 exhibits a nonlinearity based on the intensity of the incident fields, a grating profile with a $\cos^2$ dependence seemed the most logical. This dependence can be reduced to a simple sinusoidal dependence by use of the trigonometric identities. Hence, the nonlinearity of the medium and the excellent efficiency of the sinusoidal grating mesh neatly in this design. This grating can be created by propagating two plane wave pump fields at equal angles from the left and right sides of the outward pointing surface normal. Hence, the two laser beams with the proper relative phase overlap in the medium and create a sinusoidal grating of intensity dependent nonlinearity.

With the grating thus established, it was possible to examine the effect of the grating on the diffraction of a single input field to determine the relative strengths and phases of the output fields. Armed with this data, the system would be "turned around" so that the output fields become the input fields and the input field becomes the desired result. Theoretically, the only change that need be made in order to achieve this result is that the direction of propagation of all of the probe fields in the calculation be reversed. For beams with linear polarizations, this reversal of direction does not really pose much difficulty. For linear plane waves it poses no problems. However, for the reversed propagation case, a different set of computer codes was generated.

The computer codes to examine the details of laser beam combination in the reversed propagation or combining geometry were written in a slightly more general form than their forward propagation counterparts. These new versions of the propagation codes allowed for all of the effects present in the diffraction version of the codes, and also provided for variations in the relative phases of the input fields and variations in the angle of incidence of any one of the incident fields. Thus it was possible to examine the phase sensitivity of the system, demonstrating that the system was quite sensitive to the angle of incidence (maximum efficiency is halved when one incident beam deviates from the proper Bragg angle by more than 3 arcminutes), but only moderately sensitive to the relative phase of the beams (maximum efficiency is halved when the relative phase is modified by an additional phase factor $\pi/4$). Converting the latter

figure into more useful units, if the wavelength of the beam is 10.55 μm, a phase shift of $\pi/4$ amounts to a wavelength shift of 1/8 which is 1.32 μm. Hence, vibrations in the system need to be restricted to amplitudes much less than 1.32 μm.

2.3 Task 3 - Analysis of beam interaction

The simple model presented above is adequate for an introductory analysis and understanding of the basic principles involved, as well as providing a solid foundation for the initial work in grating design; however, real systems are always more complicated. The previous model does not take into account any of the more detailed effects such as beams of noninfinite extent and gaussian profiles, and makes some assumptions which are only partially fulfilled.

Inherent to the previous work is the infinite grating approximation. Gaylord and coworkers use this assumption and no attempt is made to develop a diffraction system in which the infinite grating approximation is not used. This occurs because deviation from this assumption leads to higher order evanescent waves in the analysis, which would hinder one's ability to use a simple, nonintensive numerical solution technique. An infinite grating is not present in the experimental set-up. Incident plane waves of infinite extent were assumed in our previous work to make progress in the initial analysis of the system. Changing the model to include a gaussian profile is difficult since a gaussian beam contains a distribution of propagation vectors, each of which sees a slightly different version of the diffraction grating and will be diffracted accordingly. Gaussian wave fronts are present on each of the incident laser beams.

Saturation of the medium by the pump fields leads to a significant deviation of the grating profile from the ideal sinusoidal; a nonsinusoidal grating introduces higher order propagating or evanescent waves into the system. Small perturbations of the grating profile can be tolerated since the additional frequencies present in a Fourier analysis of the modified grating profile are much larger than the number of waves present in the system. The nth Fourier component of the grating profile connects waves which are n waves apart. For example, the second Fourier component connects the 0 and +2 order waves, the -1

and +1 order waves, 0 and -2 order waves, etc. In the simple system where only two incident waves are being combined and only four incident fields are allowed to propagate, the highest Fourier component necessary is the third one. Hence, any components to the grating profile with a frequency greater than the third harmonic really can be excluded. The strength of the grating resulting from such deviations will, however, be somewhat smaller, thereby altering the effective thickness through which the beams must propagate for maximum combination to occur. Saturation effects may allow for more ingenious grating configurations which are not really sensitive to pump beam intensities but which combine several beams. Saturation effects are included in the analysis, but are avoided as an unnecessary complicating factor at present. Saturation may be present in the experiment.

It has been possible to make considerable progress using only a rudimentary model for the interaction between the pump and probe laser fields. For further work to be accomplished, more rigorous calculations with a more detailed computer code requiring a new method of solution must be developed. There is a need to include the factors mentioned above in a more fundamental fashion as well as including the effects due to the introduction of a buffer gas and thermal dissipation with the grating cell. Also, decay of the grating in time, pump and probe laser depletion, perturbations of the nonlinear medium from the steady state, use of non-steady state effects to assist in the combination, changes in the detunings of the lasers to provide lower or greater absorption, and gratings using all three dimensions should be treated.

2.4 Task 4 - Proof-of-principle experiments

2.4.1 Preliminary trials

The original plan for beam combining was to use sulfur hexafluoride (SF_6) as the medium for demonstration, to use 10P(16) carbon dioxide laser radiation for one wavelength (the pump) and either 10P(18) or 10P(14) as the probe wavelength. A cell with 7.5 cm diameter ZnSe windows spaced 1.57 cm apart was fabricated to serve as the interaction region. Partial pressures of SF_6 and a buffer gas could be independently regulated.

A simple experiment was run to attempt the observation of a grating in SF_6. The pump and probe lasers were RF-excited waveguide CO_2 lasers with cw output. The power range was roughly 1-5W TEM_{oo} and the output beams were expanded to about 1 cm $1/e^2$ gaussian diameter. The pump beam was split into two beams which then interfered in the SF_6 cell. Interference of the pump beams could be verified by replacing the cell with a fluorescent image plate. The probe beam was directed through the interference region in the cell at the calculated Bragg angle. Diffraction of the probe beam was not observed, even using a sensitive, cooled HgCdTe detector at the position expected for first order diffraction. Interaction of the pump and probe beams was observed, however. Removal of either pump or probe radiation resulted in decreased transmission of the remaining beam; this was true for various combinations of pump and probe intensities and SF_6 pressure. No buffer gas was used. All results were explainable in terms of bleaching effects. The experiments did verify some of the problems attendant with using cw CO_2 radiation, and with using closely spaced CO_2 wavelengths.

2.4.2 Design of experimental apparatus

When the decision was made to pump (create the grating) with radiation from a tetrafluoromethane (CF_4) laser in SF_6, it became necessary to create a CF_4 laser system. The objective was to use the CF_4 P(31) line at 615.1 cm^{-1} (16.26μm) to pump nearly resonant with the SF_6 Q-branch absorption which has its absorption edge[10] at 615.025 cm^{-1}. The desired output from the CF_4 laser is conveniently achieved by optical pumping with the 9R(12) line at 1073.278 cm^{-1} (9.317μm) from a CO_2 laser.[11-13] The CF_4 laser may be line tuned by changing the pump line wavelength; the desired pump/output pair happens to have a high relative efficiency.

In order to optimize the peak power available from an optically pumped CF_4 laser, a CO_2 TEA laser is commonly used as the pump. The TEA laser available for this experiment is capable of single line, multimode output of above 0.5J in a pulse of 40-50ns FWHM. But the output line of a TEA laser has a broad frequency spread because of its high pressure operation, whereas the gain cell of a CF_4 laser is typically operated at low pressure (~ a few Torr) producing a narrow absorption line. The mismatch of pump and absorption line widths leads

to inefficient energy conversion unless steps are taken to improve the width match. The preferred solution is one of narrowing the TEA laser line width by locking the output to resonant radiation already of narrow width. This may be done by including a low pressure gain cell within the TEA laser resonant cavity.

Two low pressure gain cells have been constructed for the purpose of CO_2 TEA laser line narrowing. These tubes were of the conventional pyrex construction for slow axially flowing gas mixtures (a schematic including plumbing and power connections is shown in Figure 2.4.1). O-ring sealed mounts for ZnSe Brewster windows fit on each end. Unfortunately, the CF_4 laser literature is sufficiently muddy that not all the necessary important characteristics are obvious.

The first tube was made short, with an effective gain length of about 26 cm. The short length allowed the gain tube to be mounted rigidly onto an extension of the TEA laser frame, which also held the line-selecting grating/high reflector. This action had bad consequences. It was necessary to increase the reflectance of the gain/TEA laser output coupler from 0.36 to ~0.75 in order for the low pressure gain cell to be above lasing threshold independently of the TEA gain region. The presence of radiation with the already narrow emission line width from the low pressure gain cell was essential to effectively narrow the pulsed output from the TEA laser; this was apparent from the substantial differences in 16μm energy available when the low pressure gain cell was lasing and when it was not lasing. The result of the higher reflectance output coupler was higher circulating intracavity power which damaged two gratings, one a master grating on stainless steel which was supposed to withstand such power.

Reduction of intracavity power was accomplished by returning to the R=0.36 output coupler and increasing the gain length of the low pressure cell to ~90cm, thereby allowing the low pressure cell to lase with the lower reflectance output coupler. However, this required mounting the low pressure cell and grating independently from the TEA frame, leading to undesirable long term mechanical and thermal drifts.

The inner diameter of the low pressure gain cell was chosen at a minimum value to optimize gain and restrict higher order transverse modes, but large

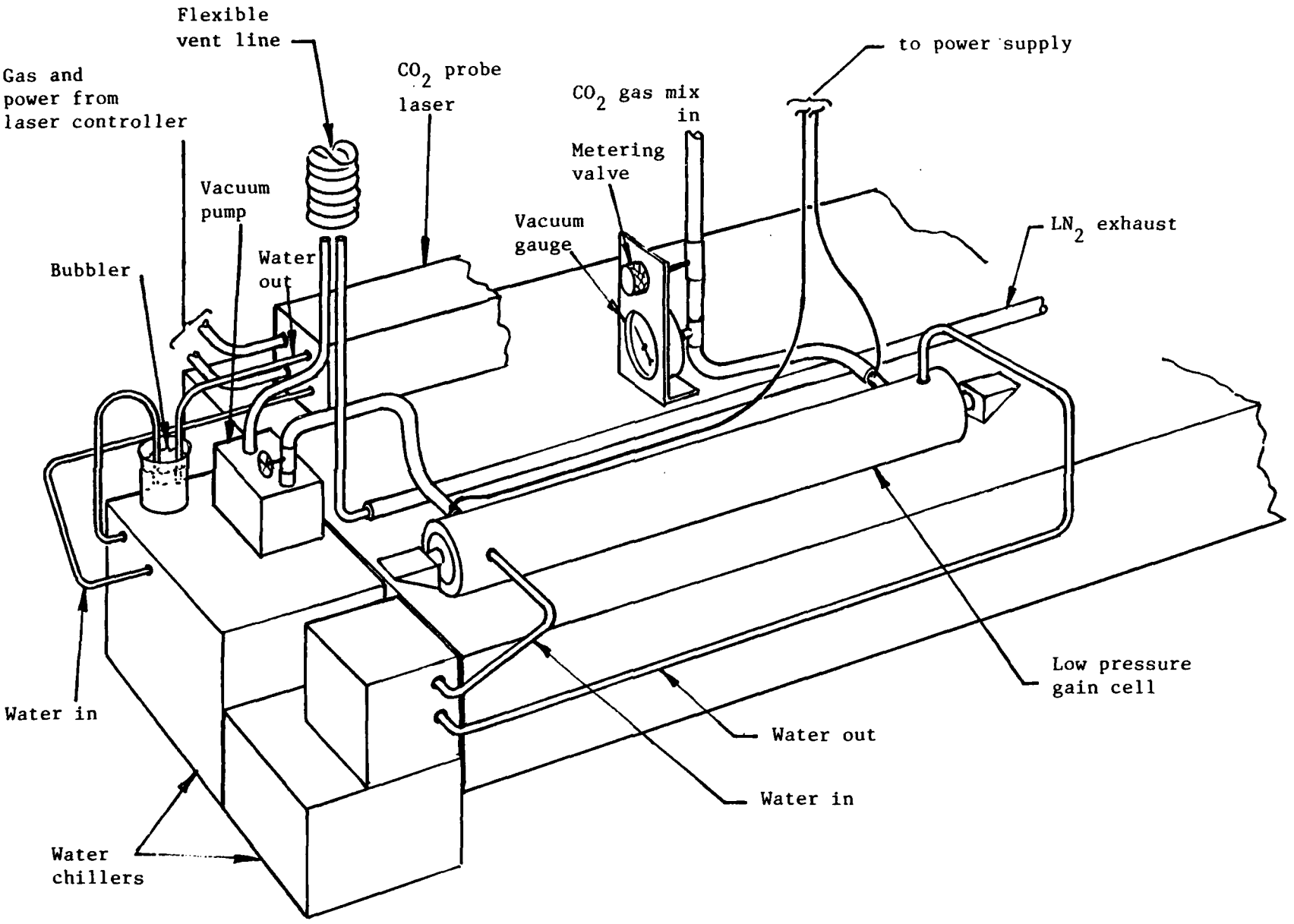

Figure 2.4.1 Plumbing schematic for flowing CO_2 lasers

enough to pass the TEM_{oo} mode with low diffraction loss. The TEA gain region has large cross section compared to the low pressure gain cell. Adjustable apertures were placed immediately in front of the cavity mirrors to aid in restricting transverse mode output to TEM_{oo}. The output coupler mirror was mounted on a piezoelectric translator which was used manually to tune cavity length over a 6μm range. The parameters of the TEA laser-low pressure gain cell cavity are given in Table 2.4.1.

The choice of inner diameter of the CF_4 gain tube was also a compromise. This dimension was large enough to pass the axially directed pump radiation and TEM_{oo} 16μm output without diffraction loss but small enough so that off-the-shelf CdTe slabs could be used as Brewster windows. The Brewster window mounts were standard design, essentially identical with those on the CO_2 low pressure gain cell. A schematic of the CF_4 laser plumbing is shown in Figure 2.4.2.

Since optically pumped CF_4 laser operation is most efficient when the CF_4 is held at temperatures below 200K, the gain tube was provided with an insulated jacket to allow circulation of liquid nitrogen. We achieved optimum operation when the measured outer cell wall temperature was about 160-165K. Figure 2.4.3 shows the percentage of pump radiation absorbed at various pressures of CF_4. The addition of helium as a buffer gas increased the absorption as shown, but also reduced the 16.26μm output; all subsequent operation of the 16μm laser was with pure CF_4 gas. Maximum output energy for the 122cm long tube occurred at 3-5 Torr indicated CF_4 pressure. The characteristics of the CF_4 laser are given in Table 2.4.2.

The geometry, separation, and wavelengths of the TEA/gain cell combination and the CF_4 laser were such that the size of the spreading TEM_{oo} mode from the TEA laser just matched the CF_4 TEM_{oo} mode size at the CF_4 back mirror/input coupler, providing a natural aperture at the back end of the CF_4 laser. At the CF_4 output coupler the pump mode was larger than the CF_4 mode; an aperture of the appropriate size placed at the output coupler helped restrict the CF_4 mode to TEM_{oo}. Very little output power was lost, and the CF_4 output seemed to stabilize after insertion of the aperture.

TABLE 2.4.1 Modified CO_2 TEA Laser Cavity

Mirror separation - 251 cm

Back mirror - flat grating, 150 lines/mm, 36°52' blaze angle

Output coupler - concave, radius of curvature = 10m
- reflectance = 0.36

Low pressure gain cell - 1.36 cm i.d.
- 90 cm gain length

TABLE 2.4.2 CF_4 Laser

Mirror separation = 152 cm

Back mirror/pump coupler - flat
- at 9.52μm, transmittance = 0.95
- at 16.26μm, reflectance = 0.82, transmittance = 0.005

Output coupler - concave, radius of curvature = 10m
- at 16.26μm, reflectance = 0.63, transmittance = 0.26
- at 9.32μm, reflectance = 0.995

Gain cell - 1.91 cm inner diameter
- 122 cm gain length

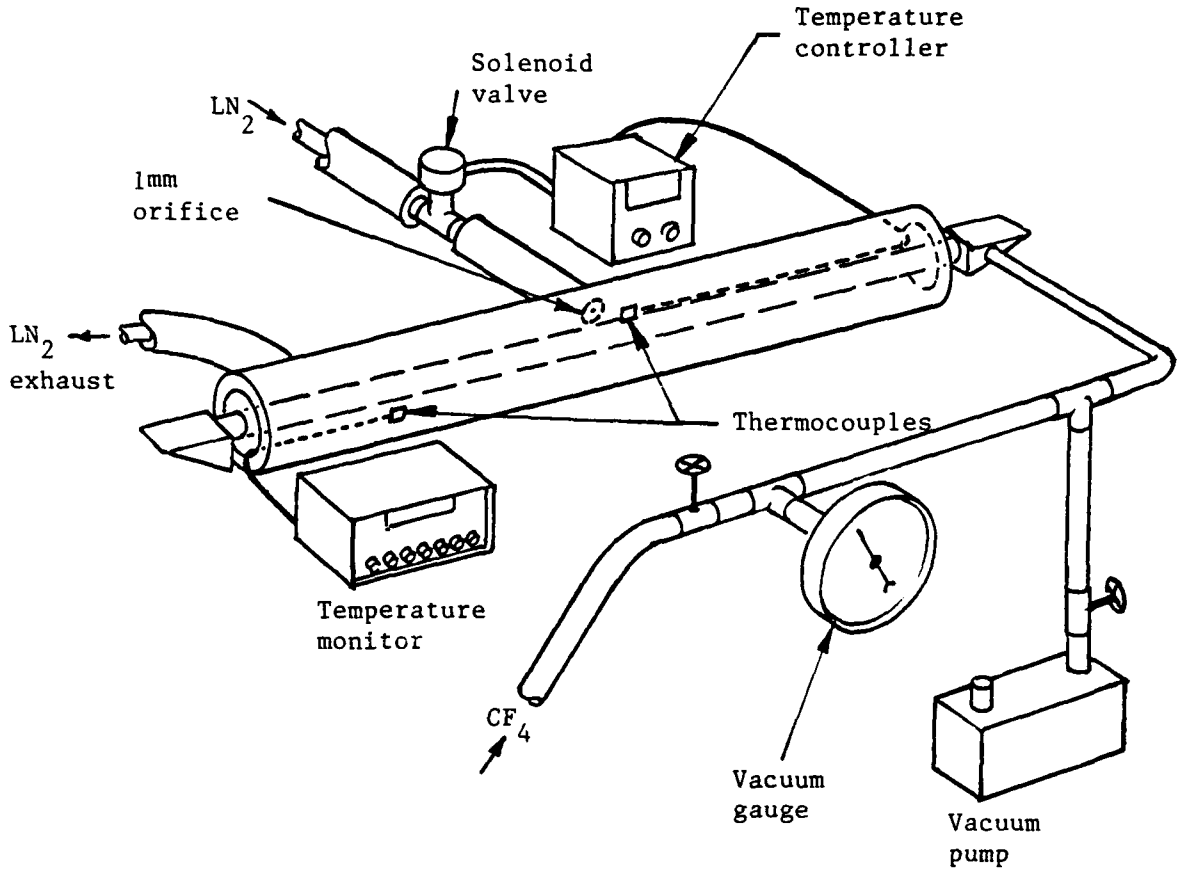

Figure 2.4.2 CF_4 laser plumbing (schematic). The 1mm limiting orifice prevents liquid nitrogen from contacting the walls of the CF_4 tube.

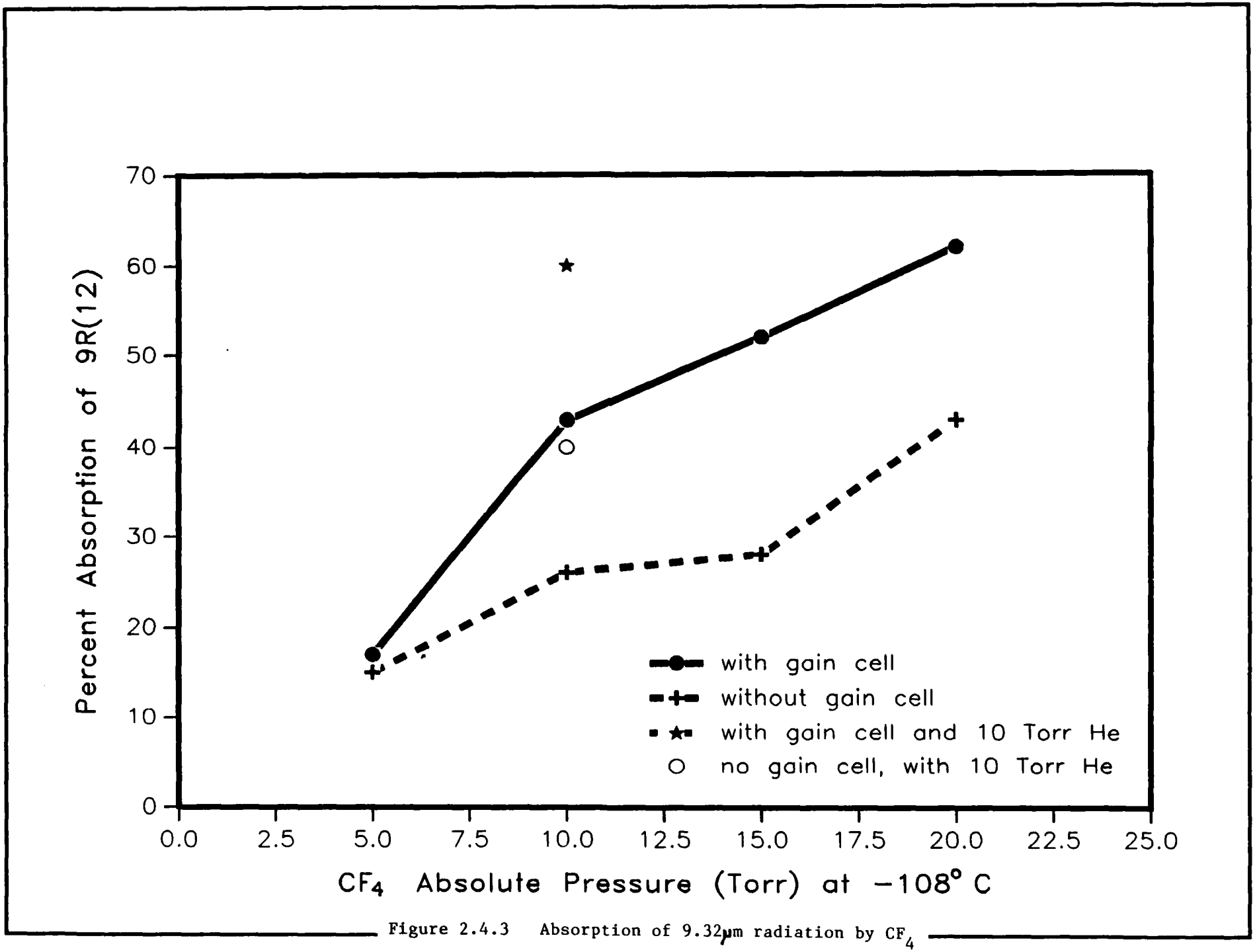

Figure 2.4.3 Absorption of 9.32μm radiation by CF_4

Although only a small percentage of the 9.32μm pump radiation came through the 16μm output coupler, the amount was comparable to the desired output radiation. Therefore another 150 line/mm grating blazed for CO_2 line operation was used to separate the 9.32μm light from 16.26μm by (nearly) retroreflecting the 9.32μm component while the 16.26μm radiation was simply specularly reflected. Beyond the grating, leakage of 9μm in the 16μm was insignificant. The highest pure 16.26μm output observed so far has been ~700μJ.

The laser that provided 10.55μm probe radiation was a low pressure, flowing gas commercial unit capable of about 25W cw TEM_{oo}. A grating provided line tunability. The laser could be converted to pulsed operation by inserting a spinning mirror Q-switch (available from the manufacturer) or by pulsing the power supply. The Q-switch was tried first, but even at TEM_{oo} operation, the laser invariably lased on two or three CO_2 vibrational/rotational lines; its use was therefore not suitable. Subsequently pulsed power supply operation was used; its characteristics will be discussed later in this report.

Again, the geometry of the overall experiment gave similar beam sizes of the 16.26μm pump and 10.55μm probe beams in the interaction region of the SF_6 cell. At the SF_6 cell, the gaussian $1/e^2$ diameter of the pump beam was calculated to be 1.16 cm; that of the probe beam, 1.23 cm.

Potassium bromide (KBr) windows were substituted onto the SF_6 cell for the ZnSe windows previously used. The cell windows are left uncoated because of the various wavelengths and angles that may be used; KBr has a low index of refraction and wide transmission range, thus reducing although not eliminating reflection losses. Since KBr is mildly hygroscopic, the cell is normally heated (to about 35-40°C) during exposure to the atmosphere, and kept in a vacuum dessicator when not in use. Figure 2.4.4 shows the SF_6 cell plumbing.

The SF_6 cell is mounted in a rotational mount which has a vernier scale; a HeNe laser defines a reference direction; this combination allows pump and probe beam entrance angles to be set to within 0.1 degree.

A schematic drawing of the setup for beam combining is shown in Figure 2.4.5; this drawing is roughly to scale. We note here that the input and output

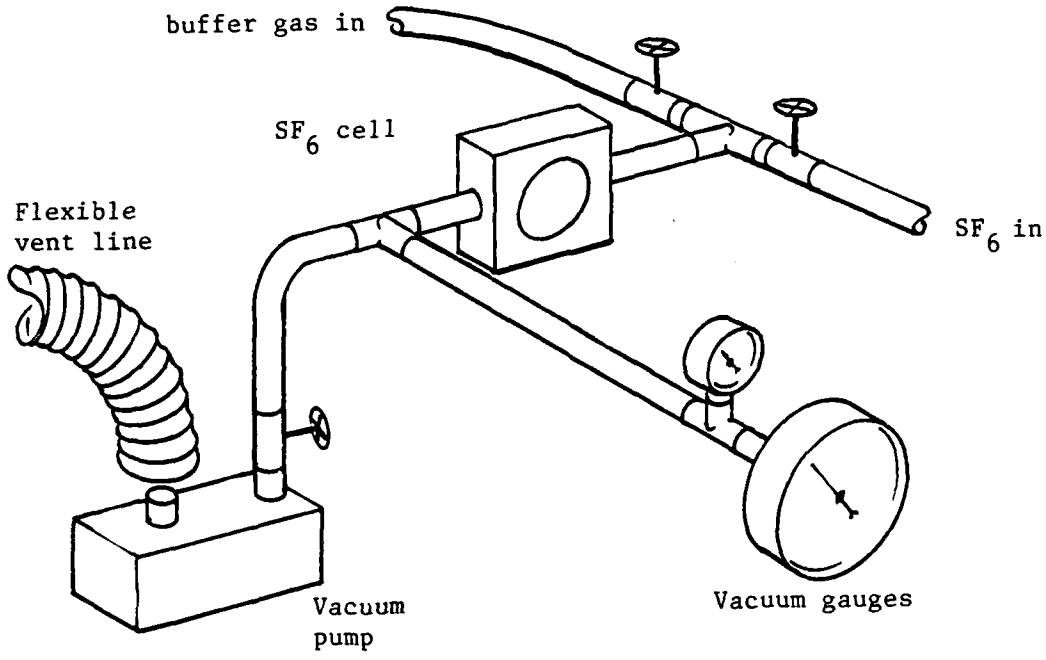

Figure 2.4.4 SF_6 cell plumbing (schematic)

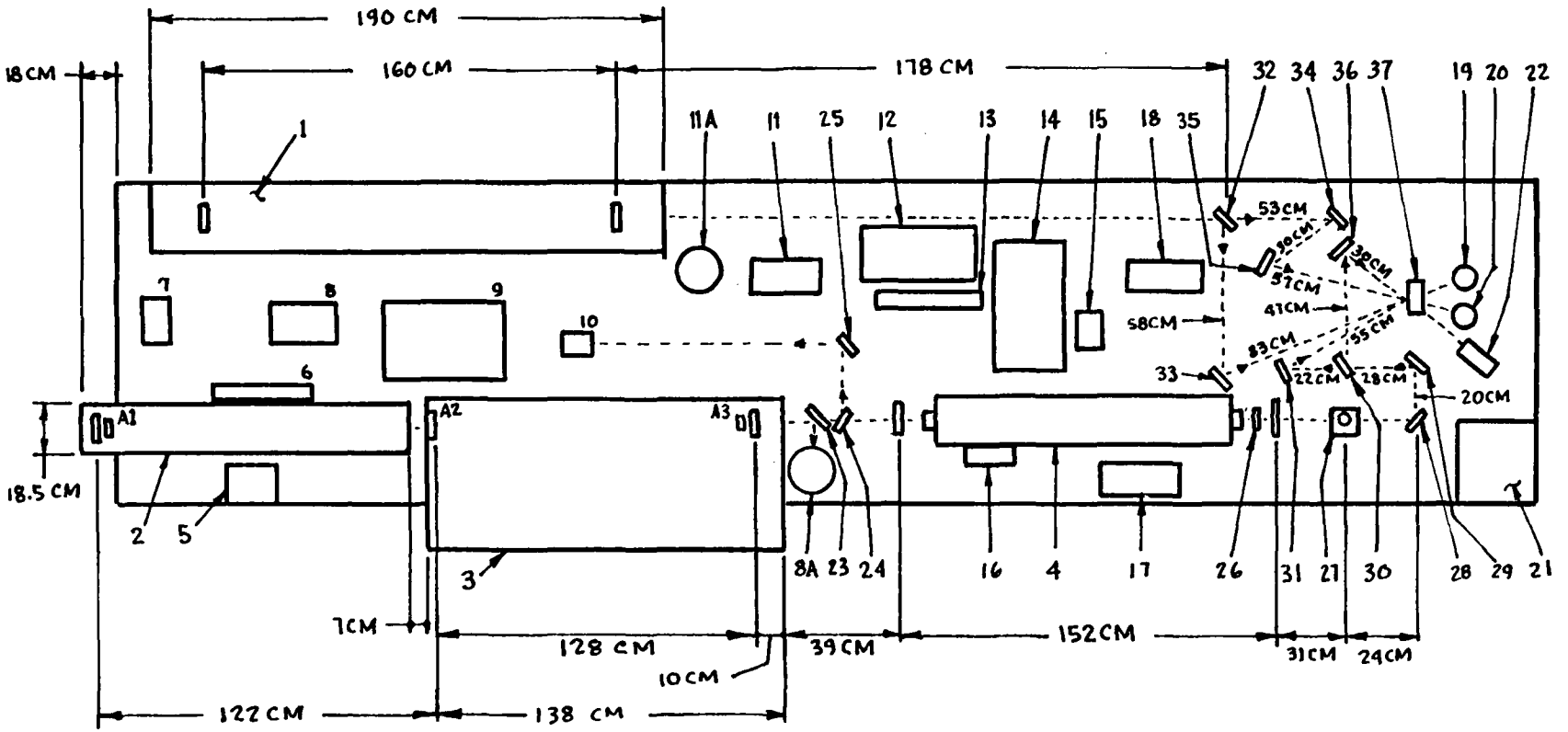

Figure 2.4.5 Schematic of experimental setup
(not to scale)

Legend for Figure 2.4.5

1. CO_2 probe laser
2. Low pressure CO_2 gain cell
3. CO_2 TEA laser
4. CF_4 laser
5. HeNe power supply
6. HeNe laser - CF_4/TEA alignment; uses two mirrors (not shown)
7. Vacuum gauge for gain cell
8. Power meter readout

8A. Power meter head

9. Spectrum analyzer - CO_2 lines (pump)
10. Pyroelectric detector - 9.3μ pulse monitor
11. Power meter readout

11A. Power meter head

12. HeNe power supply
13. HeNe laser - SF_6 cell centerline
14. Spectrum analyzer - CO_2 lines (probe)
15. Temperature controller - CF_4 tube
16. Temperature readout - CF_4 tube
17. Vacuum gauge - CF_4 tube
18. Vacuum gauge - SF_6 cell
19. 10.55μ detector - HgCdTe
20. 10.55μ detector - HgCdTe
21. Radiometer readout
22. Radiometer head - 16μm
23. Beam splitter - TEA to power meter
24. Beam splitter - TEA to pyroelectric detector
25. Turning mirror
26. Aperture
27. Beam raiser/9.3μ leakage rejection grating - 2cm height change
28. Turning mirror
29. Turning mirror
30. Beam splitter
31. Turning mirror
32. Beam splitter
33. Turning mirror
34. Turning mirror
35. Turning mirror
36. Turning mirror
37. SF_6 cell

A1, A2, A3 - apertures

couplers for the CF_4 laser, and the 45° 50/50 16μm beam splitter were designed and fabricated at LTV for this program. Photographs of the apparatus, taken from various angles, are shown in Figures 2.4.6 - 2.4.11.

2.4.3 Experimental results

A two step overall approach was taken to reach the goal of demonstrating beam combining. The first step was to demonstrate that 16.26μm pump radiation could write into SF_6 a grating that would diffract a single 10.55μm probe beam. Once the grating had been demonstrated, it was intended to further characterize the grating with a single probe beam by varying SF_6 pressure and pump intensity, and then checking the effect, if any, of varying the probe beam intensity. Having done grating characterization, the second step would be to examine beam combining, to explore the relation between pump and probe intensities and powers, to begin to push toward high probe intensities.

After assembling the apparatus, a rough cut first experiment was done to demonstrate the presence of a grating. SF_6 pressure was set at 0.1 Torr and helium was added so that total pressure in the cell was ~18 Torr. A single cooled HgCdTe detector looked at the zero order, or direct transmitted probe pulse. No reduction of the zero order was observed during the time the pump pulse was on; that is, no grating was observed.

Before the second trial, the general alignment of the experiment was improved, and a second cooled HgCdTe detector was placed to look at the first diffracted order of the probe beam. The probe beam width and the acceptance aperture of this detector should have accommodated small errors in positioning, and small changes in position of the pump beam. The pump/probe pulse timing was reset so that the pump pulse (~50ns FWHM) appeared 5-8μs after initiation of the probe pulse (~75μs FWHM). The output of both zero and first order detectors were examined during the pump pulse; again, no diffraction was observed for variation of the SF_6 pressure from 1 to 9 Torr, with total cell pressure set at ~16 Torr (the balance was again helium). At each pressure, the pump angle was swept in small steps through an angle ~0.73° around the calculated Bragg angle because of the predicted sensitivity to the setting of the Bragg angle.

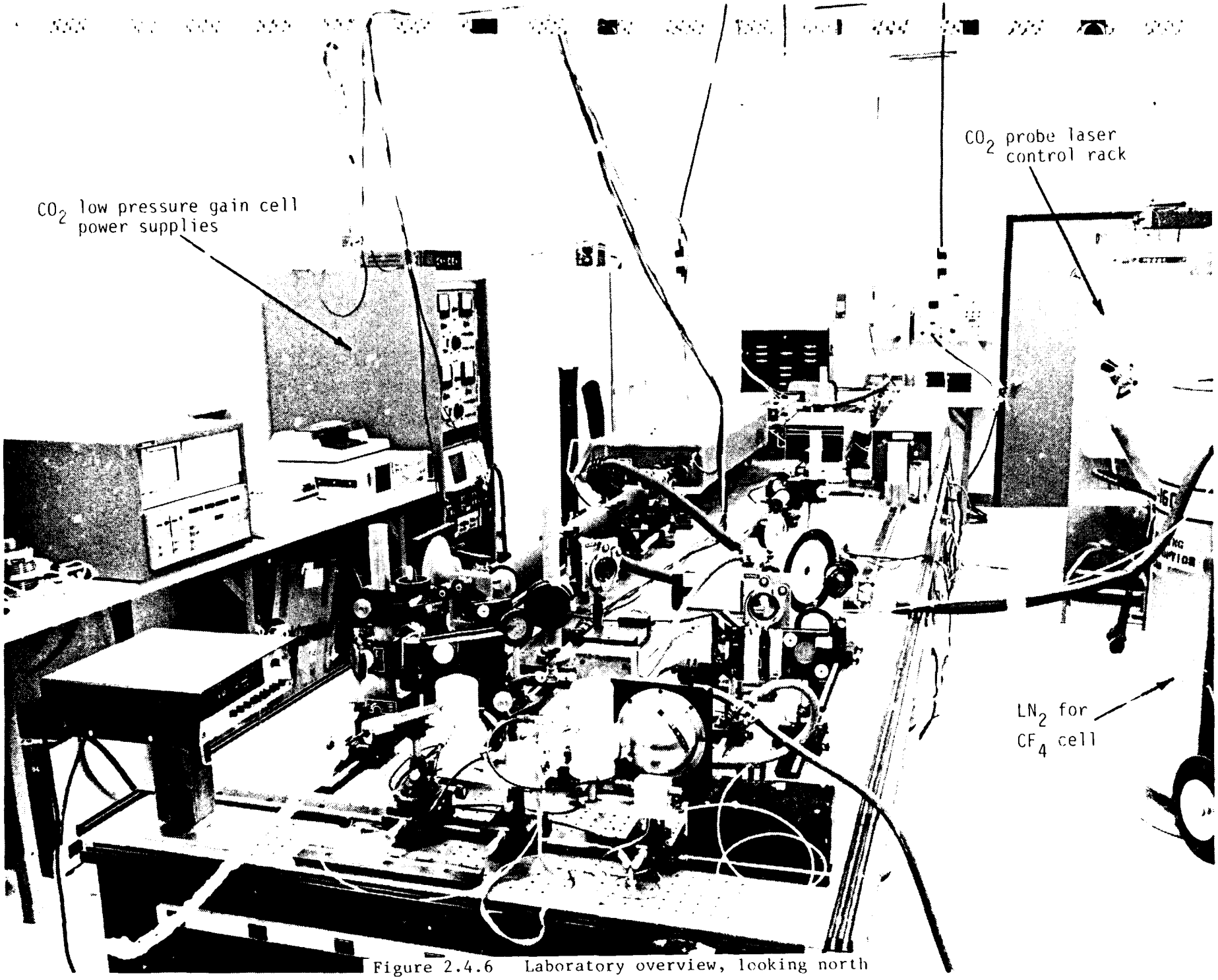

Figure 2.4.6 Laboratory overview, looking north

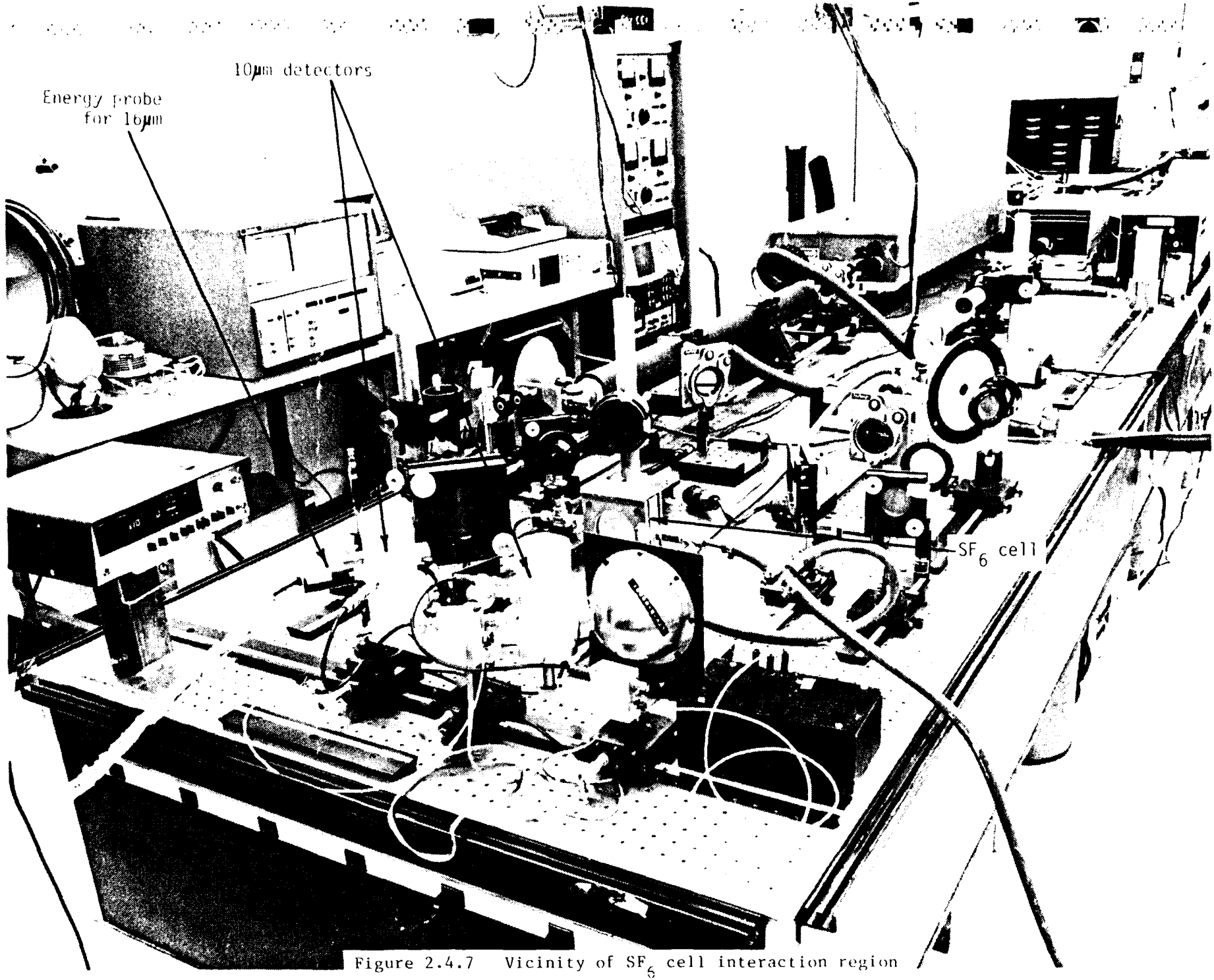

Figure 2.4.7 Vicinity of SF_6 cell interaction region

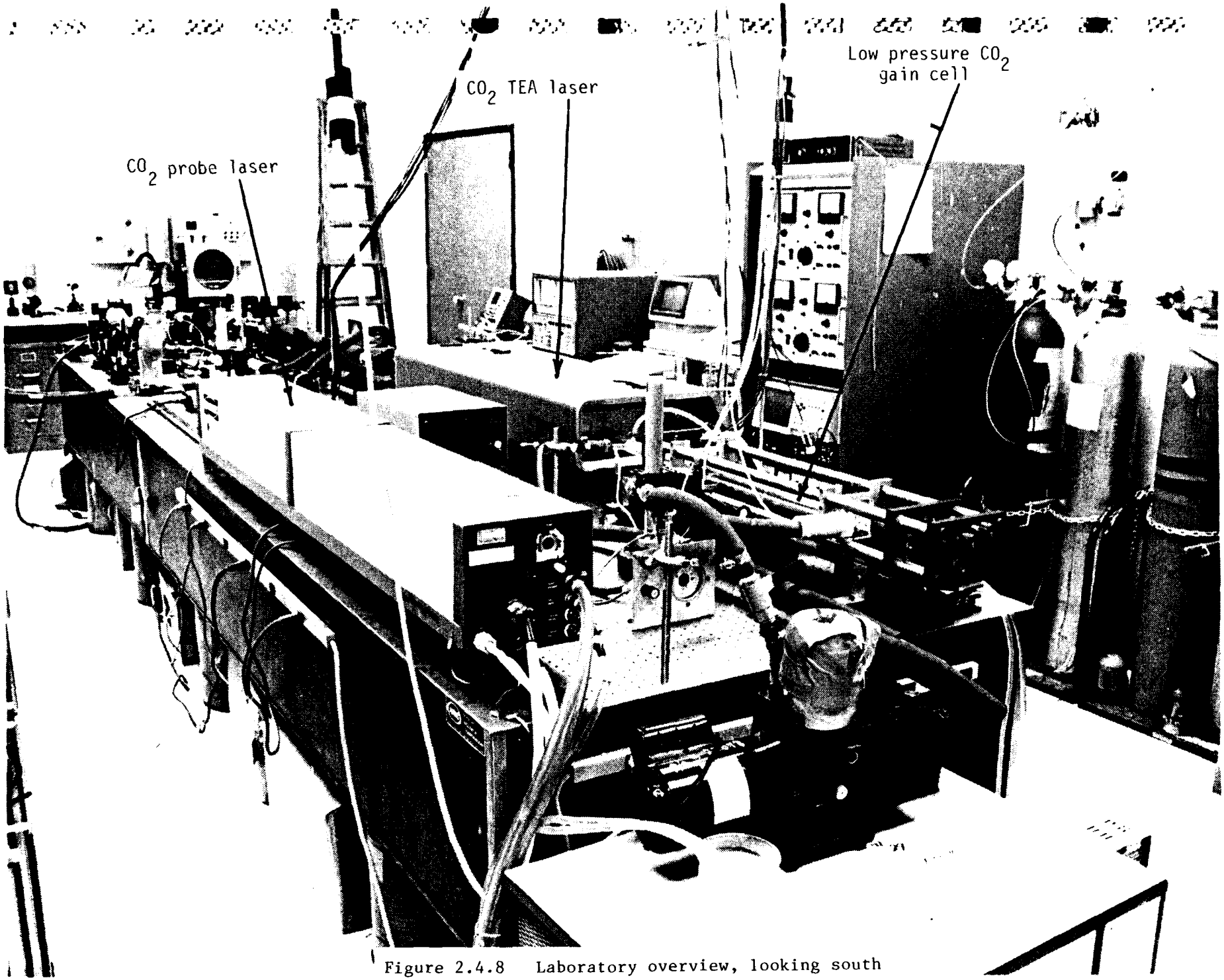

Figure 2.4.8 Laboratory overview, looking south

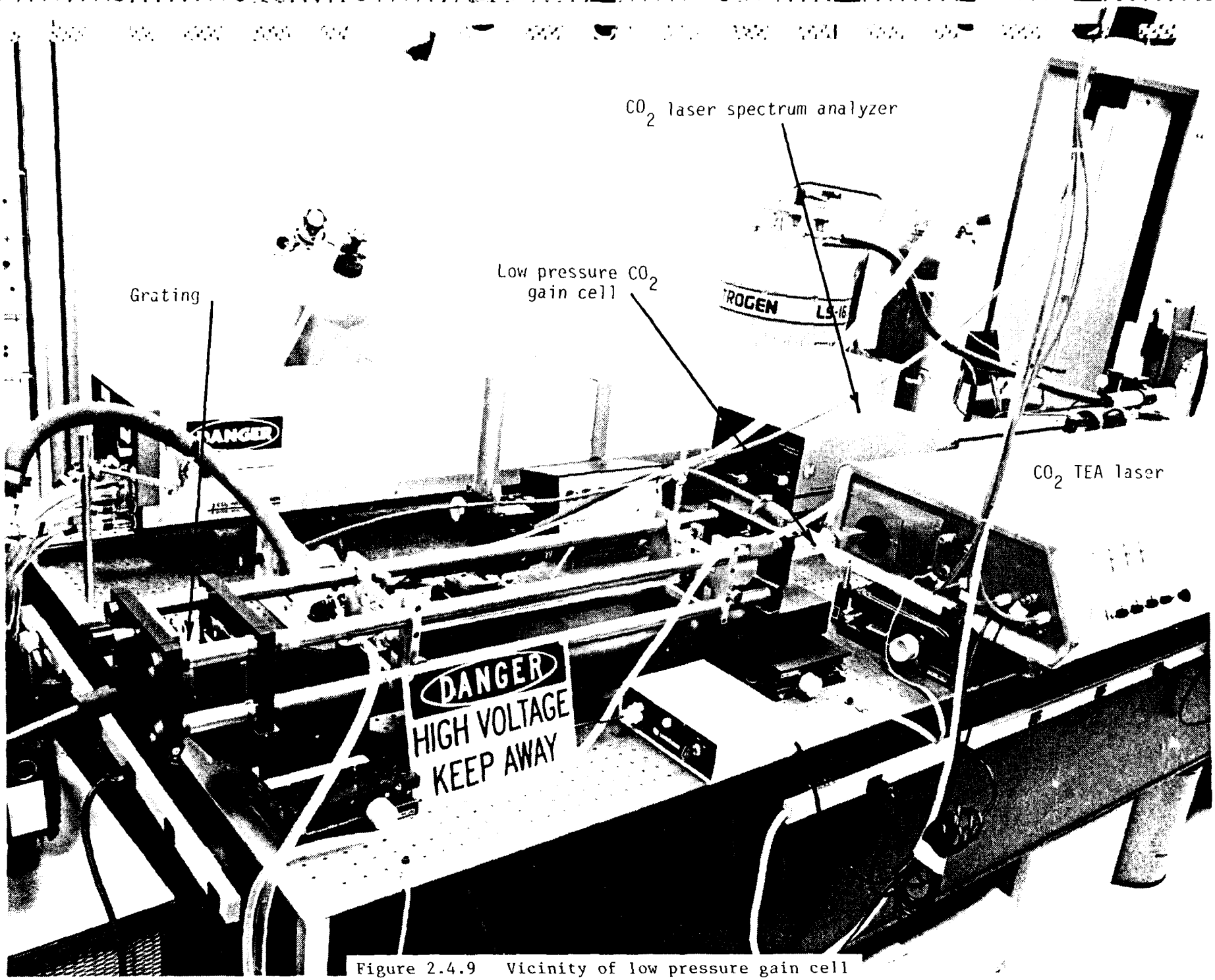

Figure 2.4.9 Vicinity of low pressure gain cell

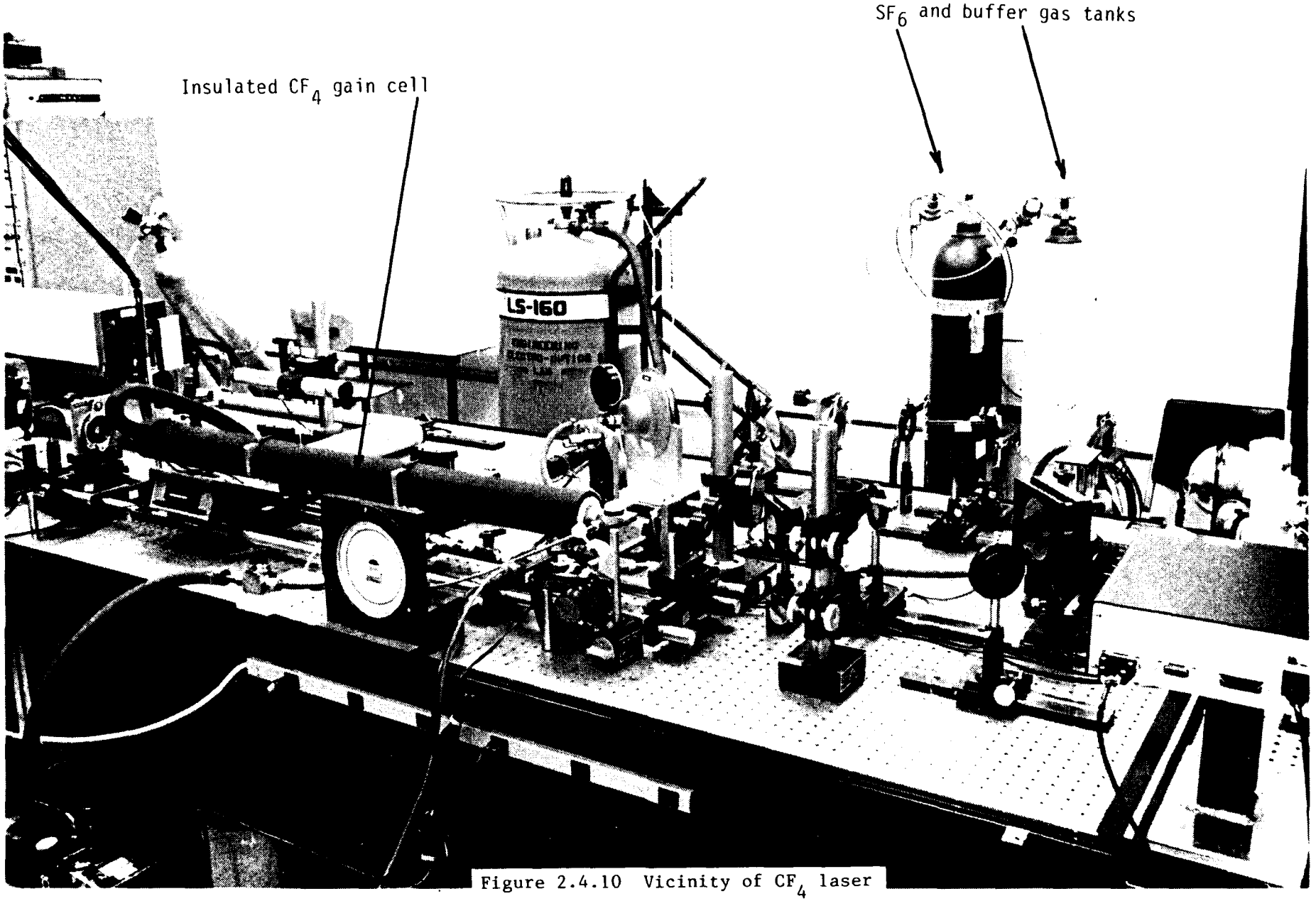

Figure 2.4.10 Vicinity of CF_4 laser

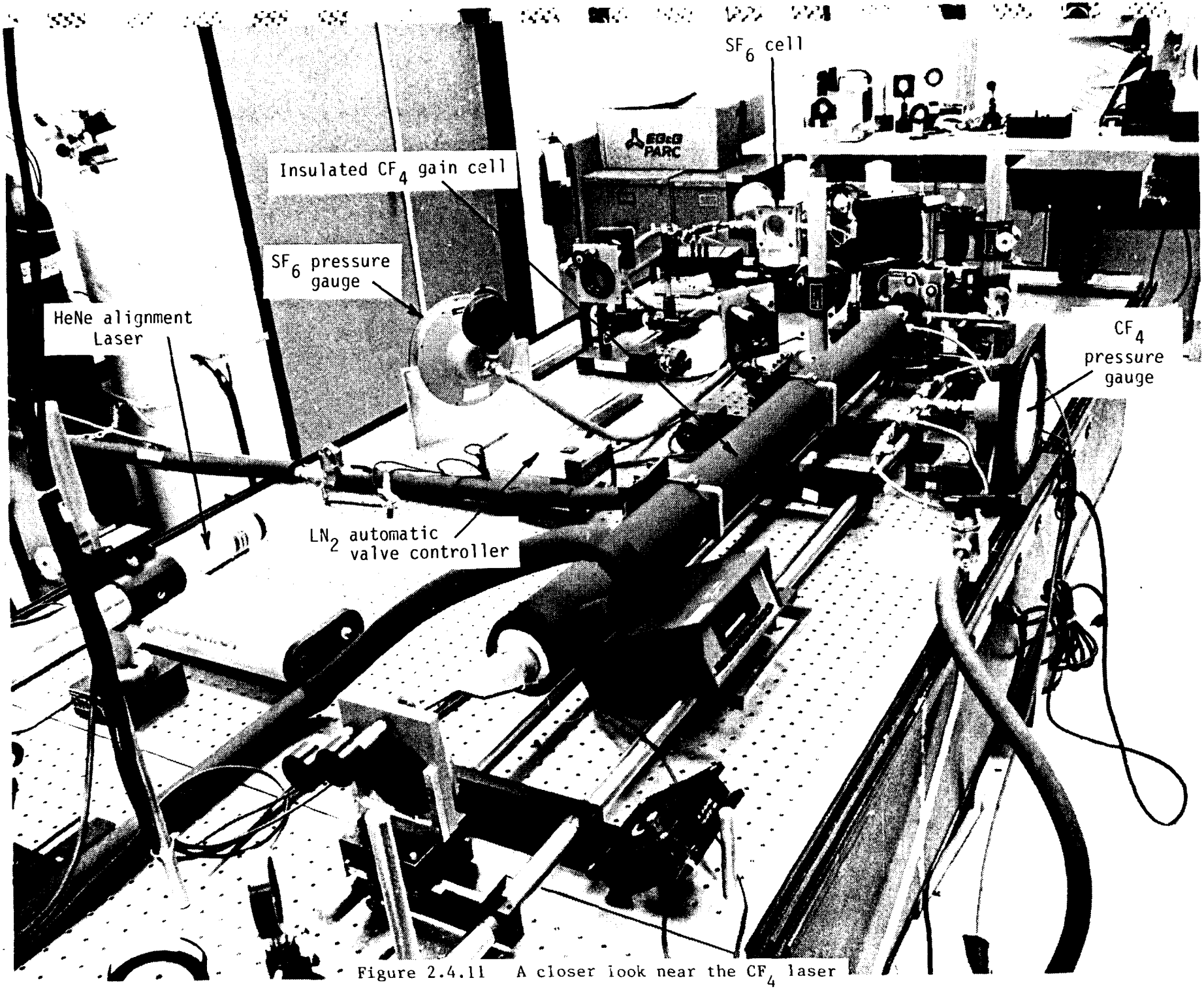

Figure 2.4.11 A closer look near the CF_4 laser

At this point a first hand examination of some of the absorption data used in the theory seemed to be in order. The 10.55μm absorption in pure SF_6 was checked first. Since the apparatus was set up for calculated Bragg angle incidence, the path length through the SF_6 was ~1.57/cos 19° = 1.66 cm. The data taken is shown as "first" in Figure 2.4.12. The measured absorption coefficient was 0.16 cm^{-1} $Torr^{-1}$ for low pressure ($\leq$1.6 Torr); the value used in Section 2.2 is 0.4 cm^{-1} $Torr^{-1}$.

We next measured 16.26μm absorption; data for pure SF_6 is given in Figure 2.4.13. The data presented in this and subsequent absorption plots was not normalized (thus the arbitrary ordinate scale); what is plotted for the ordinate variable is a ratio of detector readings, (transmitted sample)/(incident sample). The multimode data appears to be a gentle curve, the single mode data seems to have two slopes, with a break near 12 Torr SF_6 pressure. The absorption below 12 Torr is 0.049 cm^{-1} $Torr^{-1}$; above 12 Torr, 0.072 cm^{-1} $Torr^{-1}$. The absorption path was 1.81 cm since the angle of incidence was 30°. The break in the absorptance at 12 Torr is not understood at this time.

Data for absorption of 16.26μm radiation in SF_6 in the presence of helium is shown in Figure 2.4.14. For each data point, the pressure was set by evacuating the cell, admitting SF_6 to its desired pressure, then filling with helium to a total pressure of 18 Torr. Although the data is somewhat scattered (as evidenced by the zero pressure data points), there appears to be only a very slow decrease in transmission until SF_6 pressure is above ~15 Torr, where substantial absorption takes hold. In a variation of the procedure just described, SF_6 pressure was varied again from 0 to 17 Torr, but this time helium was added to give a total pressure ~250 Torr. In the latter experiment, within the data scatter, no 16.26μm absorptance at all was observed; transmission of 16.26μm through the cell with 250 Torr of helium (with or without SF_6) was identical to transmission of an empty cell!

A further experiment was run to check the previous surprising result. SF_6 pressure was set at 7.5 Torr and varying amounts of helium were added; the data are given in Figure 2.4.15. SF_6 at 7.5 Torr (for our absorptance path) without any helium absorbs about half of the incident 16.26μm radiation (compare with Figure 2.4.11), while addition of helium <u>reduces</u> the 16.26μm absorption. The

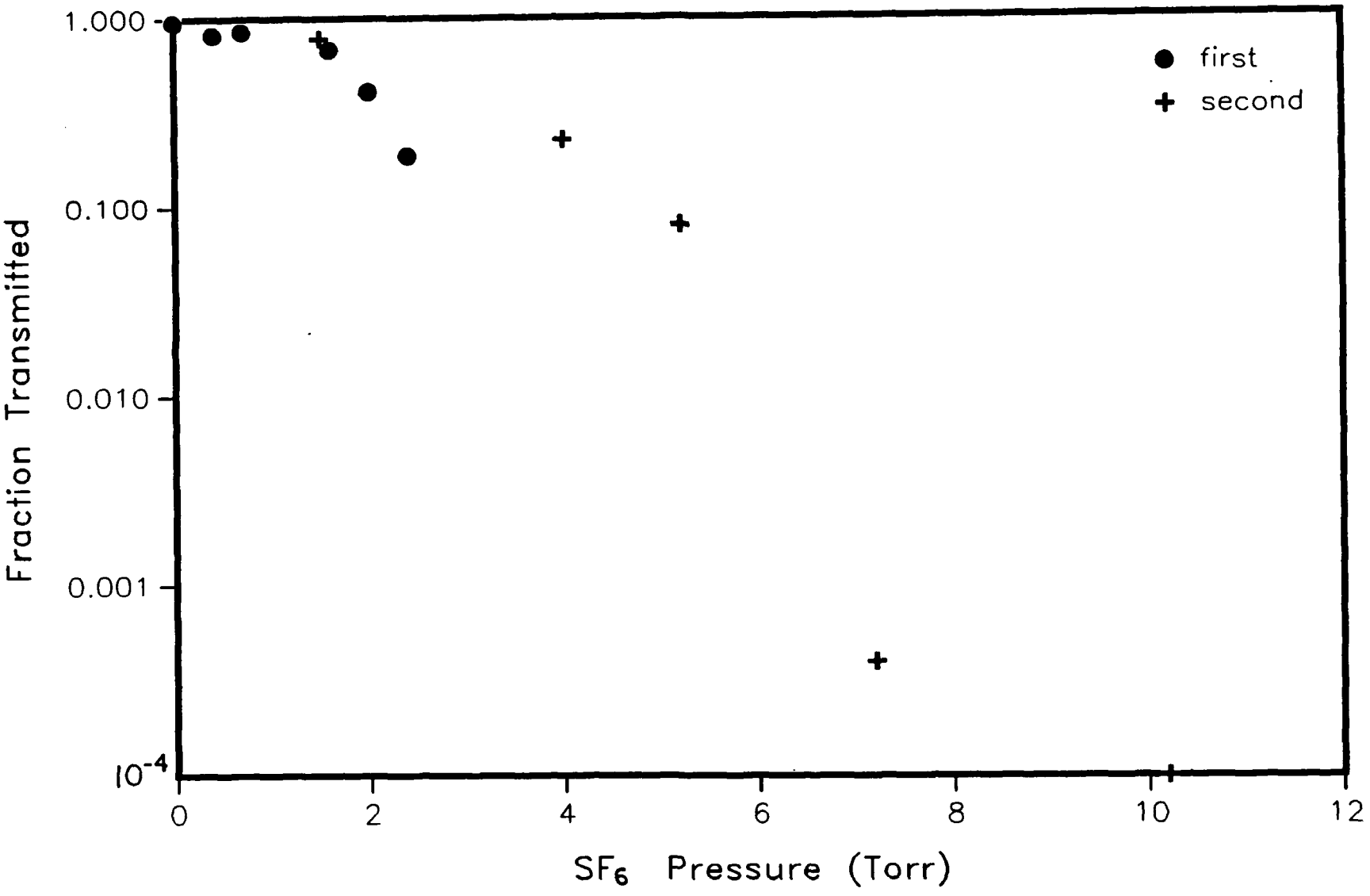

Figure 2.4.12 10.55μm absorption in pure SF_6

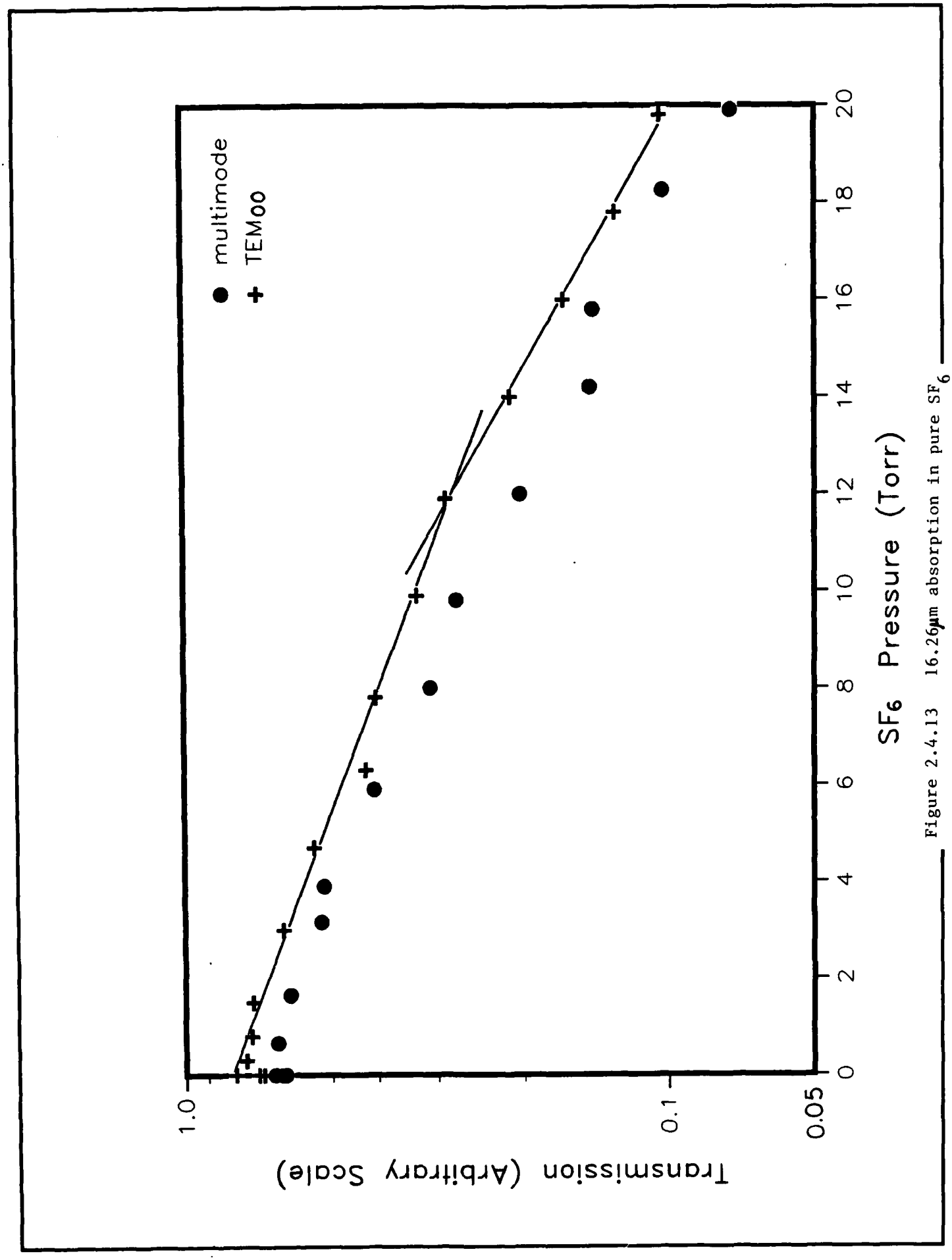

Figure 2.4.13 16.26μm absorption in pure SF_6

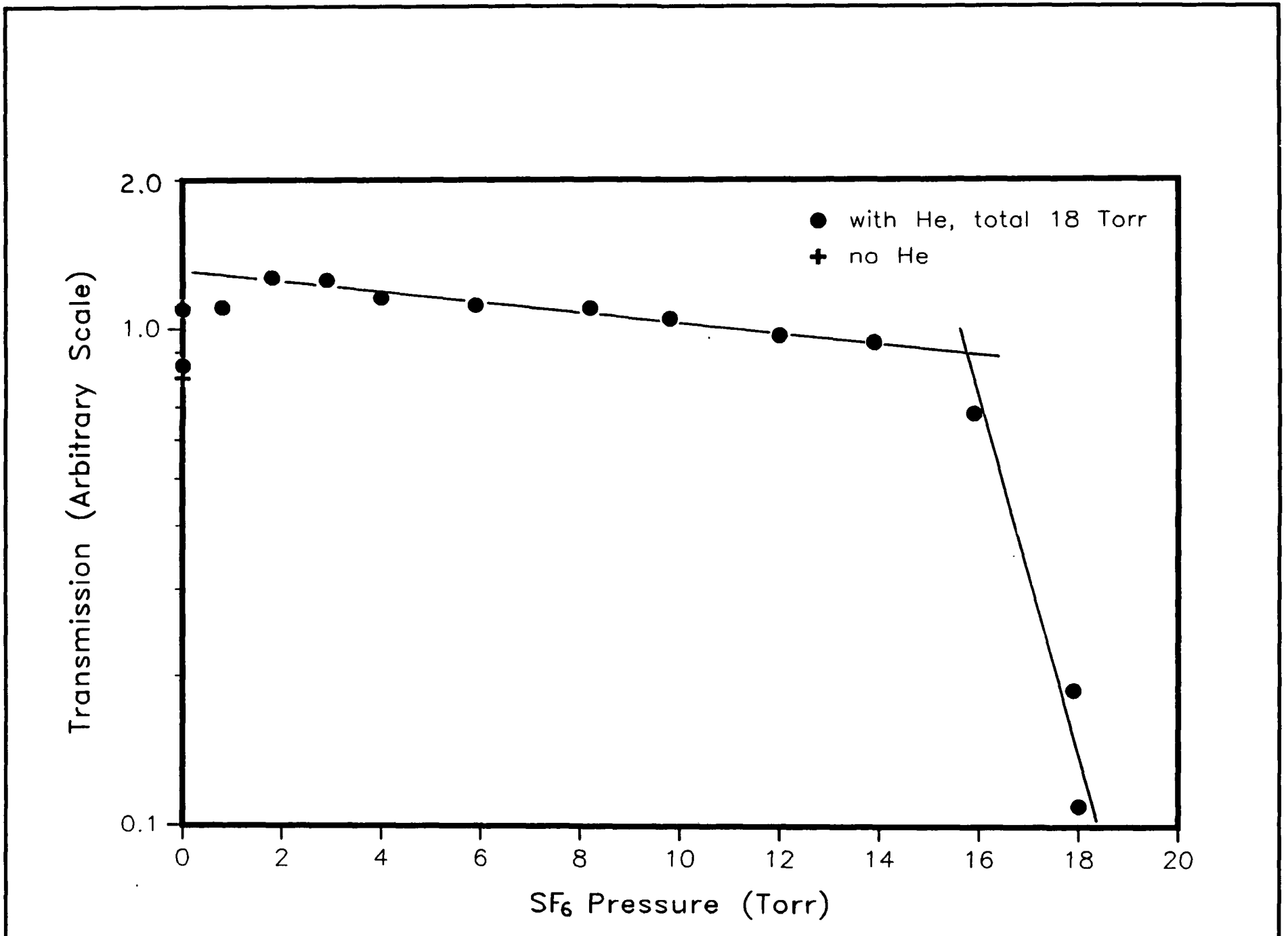

Figure 2.4.14 16.26μm absorption in SF_6 with He

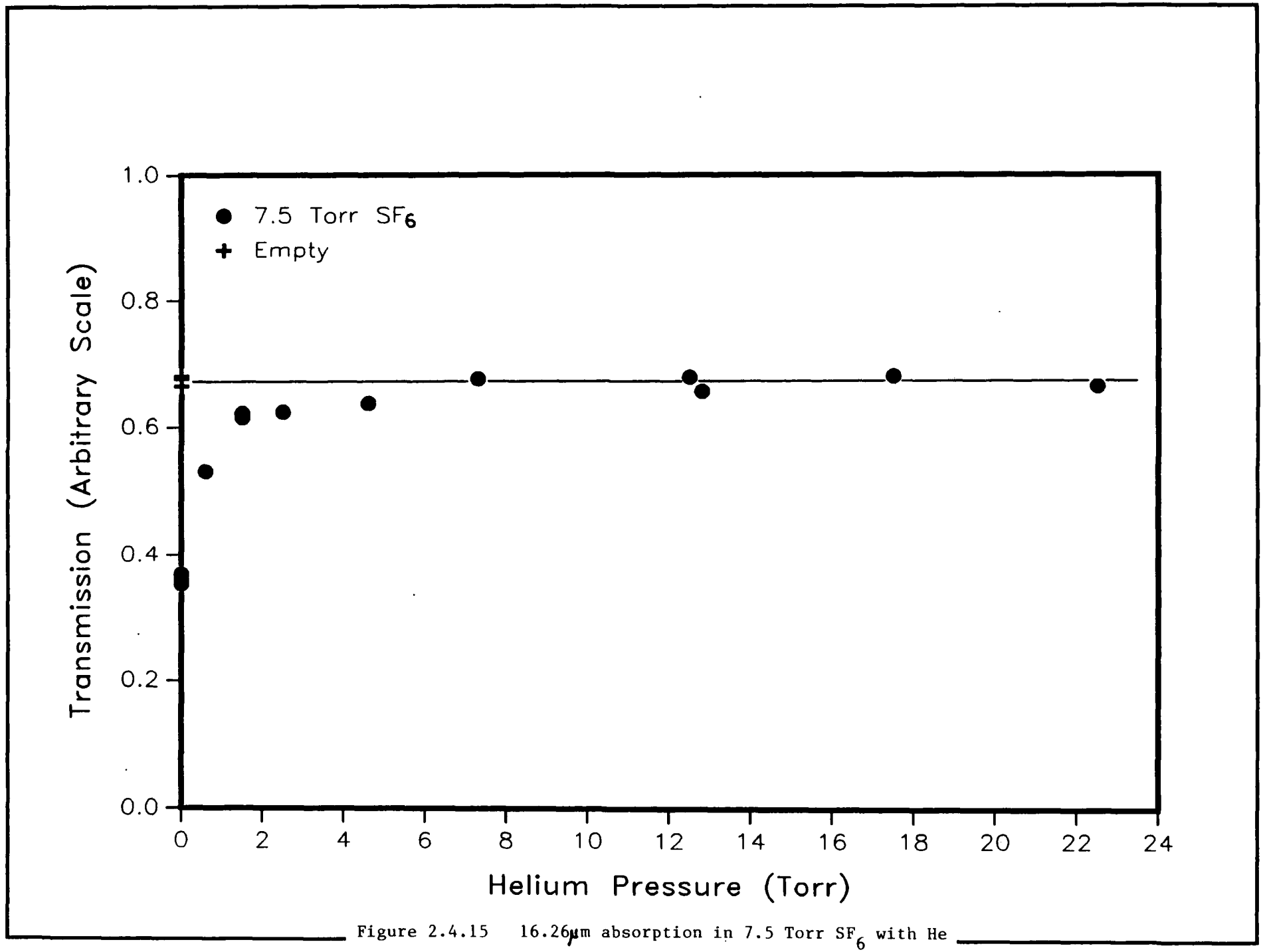

Figure 2.4.15 16.26μm absorption in 7.5 Torr SF_6 with He

break seems to occur at about 2-3 Torr, and this agrees well with the data of Figure 2.4.12, in which substantial 16.26μm absorption occurs only when helium pressure has been reduced to less than 2-3 Torr of the total pressure. Thus we see that addition of small amounts of helium into SF_6 gas renders SF_6 partially to totally transparent to 16.26μm radiation!

For the moment allowing the reasons for the SF_6/He interaction to go unquestioned, we returned our attention to grating demonstration. Absorption data for 10.55μm in SF_6 without helium was rerun to try to find a compromise value of pressure at which there would be some absorption at both 10.55 and 16.26μm, but enough transmission at 10.55μm to have a chance to see diffracted radiation. Here the data marked "second" in Figure 2.4.10 was taken. A pressure of 5.5 Torr SF_6 was selected; of course no helium would be added.

One further refinement was added to the apparatus: a differential micrometer was placed on the mirror mount controlling the angle of incidence of the probe beam to the sample cell. The coarse scale allows a finer step than previously available for sweeping through the Bragg angle, and the fine scale would allow adjustments less than $\pm 0.01°$ should a grating be observed.

The search-for-grating experiment was rerun as described above. The probe angle of incidence was moved in small steps such that the half power points of the probe beam were not allowed to go outside the half strength points of the grating. The angle was reset three times to give a total range of swept incident angle of 1.4°. Once again, no energy was observed at the first order position.

What <u>was</u> observed during the search-for-grating experiment at 5.5 Torr SF_6 pressure was a change in the shape of the 10.55μm pulse after passage through the SF_6 cell, a change that had not been seen at lower operating pressure. This observation prompted a closer look at 10.55μm transmission through SF_6. The following data were obtained by sampling the incident and transmitted beam signals with a fast digitizing oscilloscope and displaying the digitized signals after capture on an X-Y pen printer. The "incident" detector views a portion of the incident beam (from a beam splitter) through an integrating sphere. The "transmitted" detector views the beam transmitted through the SF_6 cell through a

CaF_2 attenuator where appropriate; since we were interested in shape of pulse and time relationships, no attempt was made to determine absolute intensities.

Pulse transmission data taken at 2 Torr SF_6 pressure are shown in Figures 2.4.16 and 2.4.17. These are characteristic of data taken at this or lower pressure, or with no cell. It is seen that the FWHM of the main part of the power-supply-switched pulse is about 100μs. Apparently the spike at the front edge is a gain-switched Q-pulse; its FWHM on the 5μs/div trace is measured at 579 ns for either incident or transmitted signal. Also, the peak-to-valley ratio for the valley immediately following the Q-pulse is the same (4.66) for both incident and transmitted signal. That is to say, for SF_6 pressures 2 Torr or below, 10.55μm radiation of the intensity available to us is transmitted through SF_6 with pulse shape basically unchanged. The transmitted pulse sometimes shows high frequency modulation not seen on the incident pulse. We have not yet determined the source of this modulation; possible candidates include longitudinal mode competition in the laser (masked from the sampled incident beam by the integrating sphere), etalon effects in the cell, or ringing in the electronics.

10.55μm pulse transmission through SF_6 taken at pressures above about 4 Torr are shown in Figures 2.4.18 - 2.4.24. The outstanding feature of this data is the apparent delay of the pulse transmission. From the data shown, delays of 20-30μs can occur. In some cases, the transmission responds in steps (Figures 2.4.20 and 2.4.22); the first Q-pulse is transmitted, but the SF_6 responds again to a minor spike in the incident pulse, as if overcoming a threshold effect.

Sulfur hexafluoride, of course, is known to interact strongly with CO_2 laser radiation. It was one of the first materials to be used as a saturable absorber passive Q-switch for the CO_2 laser.[14] Furthermore, self induced transparency, which occurs as a result of the coherent coupling of a laser beam with an absorbing system, also affects the passage of CO_2 laser radiation through SF_6.[15,16]

The question immediately arises as to whether similar effects take place when a 16.26μm pulse is incident on SF_6. With the detectors on hand for 16.26μm at the time (pyroelectric energy meters), it was not possible to investigate 16.26μm transient behavior.

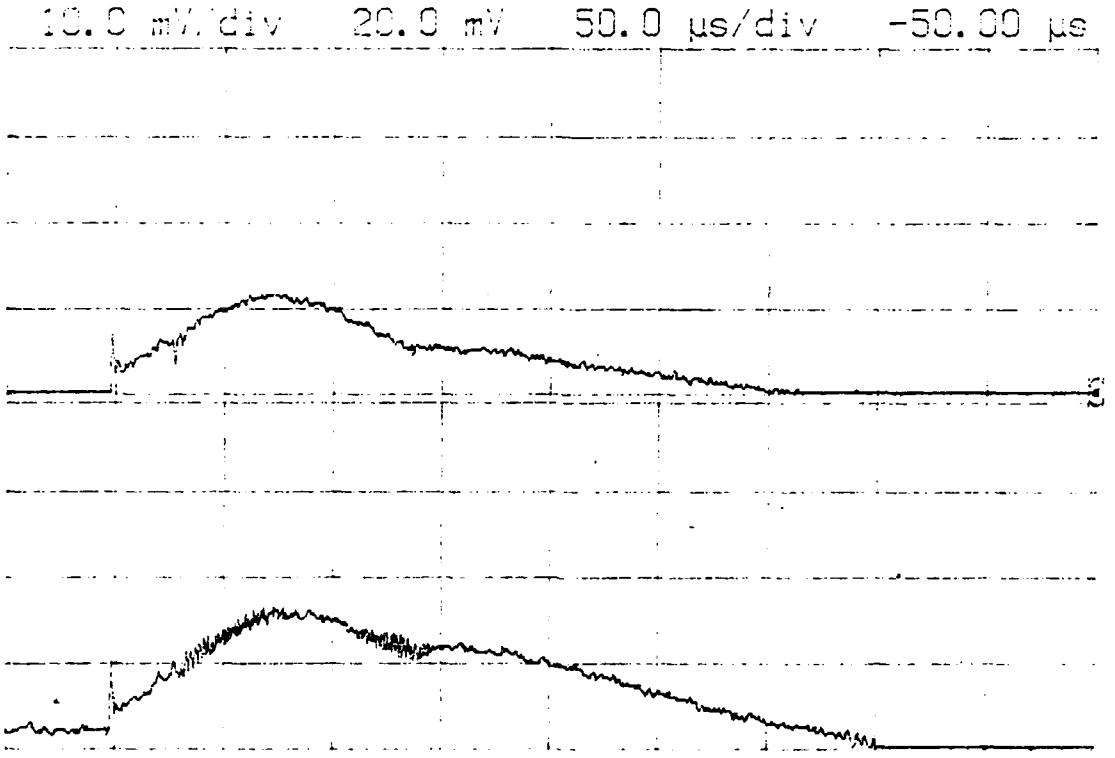

Figure 2.4.16 10.55µm pulses incident on (top) and transmitted through (bottom) 2.0 Torr SF_6

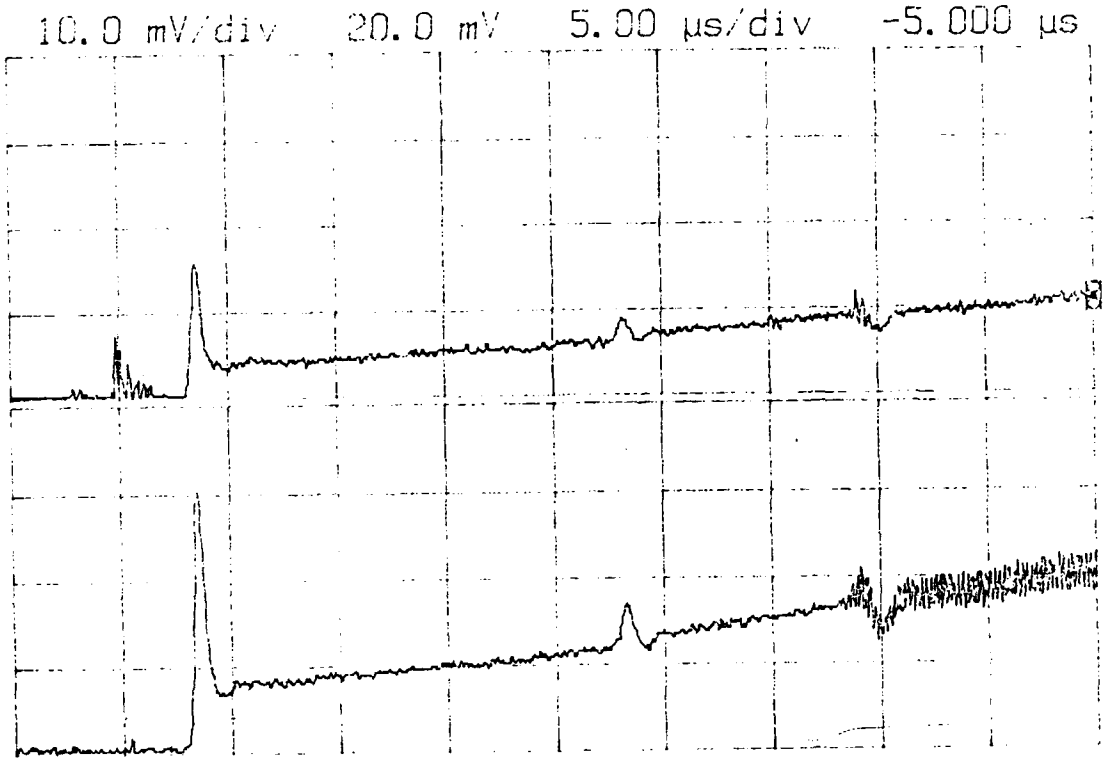

Figure 2.4.17 SF_6 pressure: 2.1 Torr. The transmitted pulse is in phase with the incident pulse, and reproduces its features.

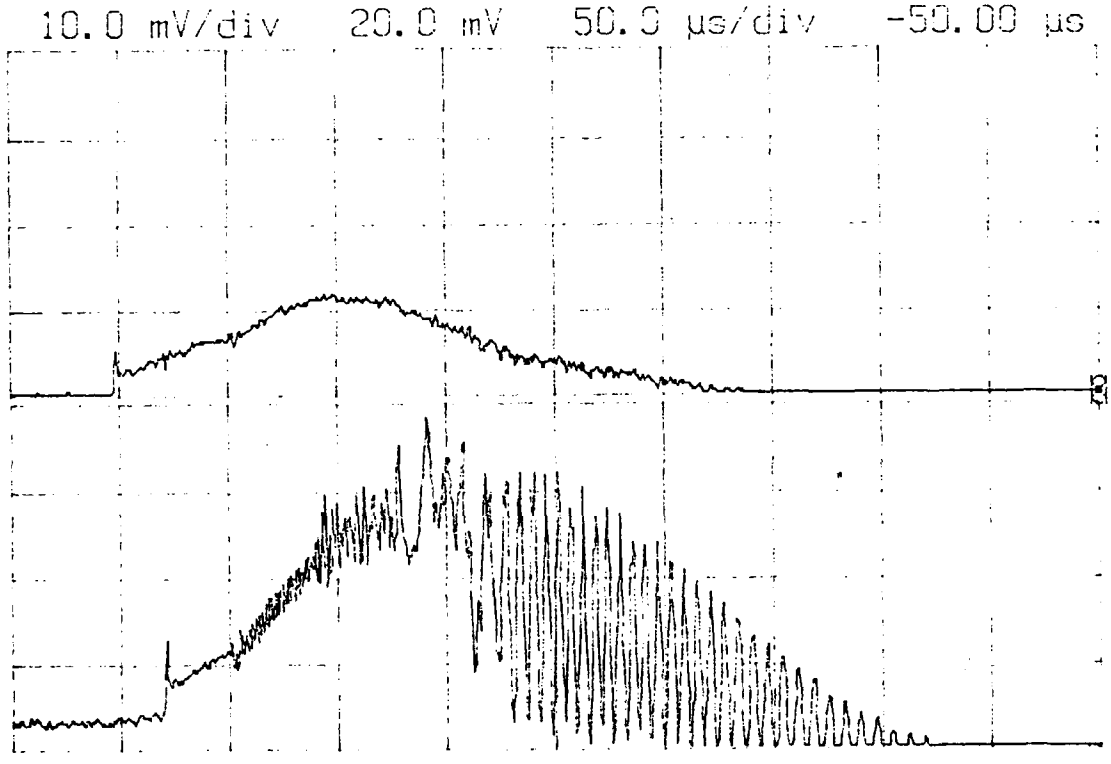

Figure 2.4.18 SF_6 pressure: 5.1 Torr. The transmitted pulse is delayed about 20µs from the incident pulse.

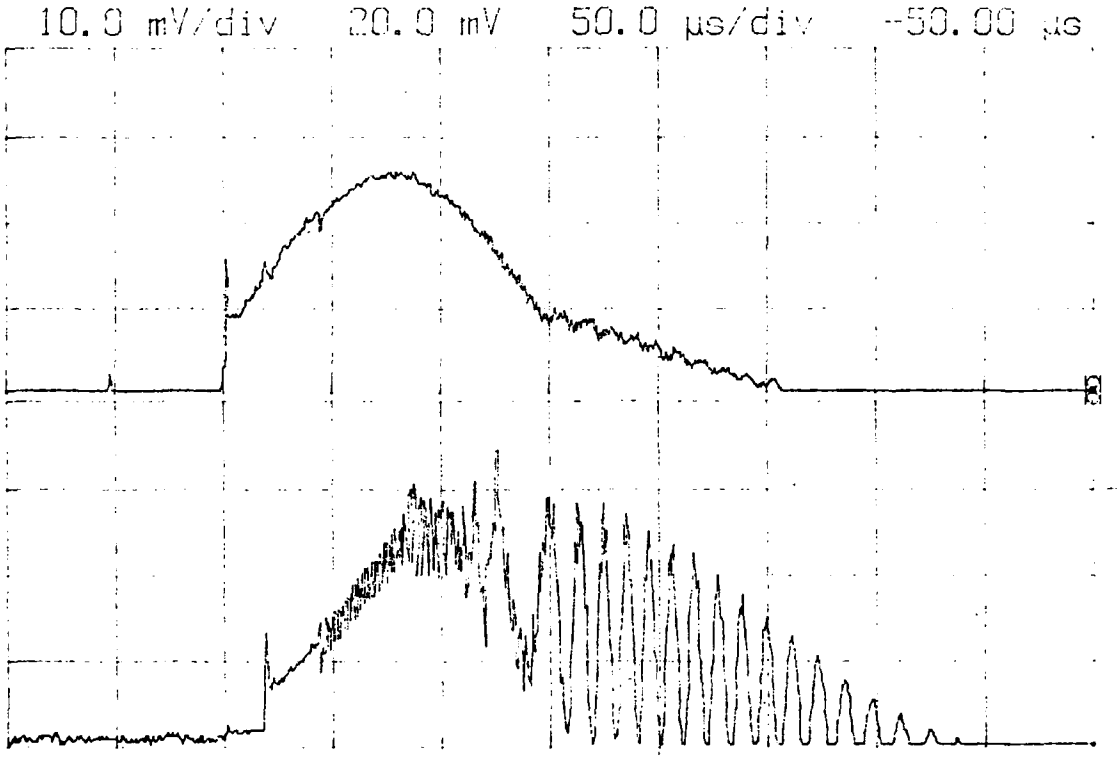

Figure 2.4.19 SF_6 pressure: 4.3 Torr. Again about a 20µs delay.

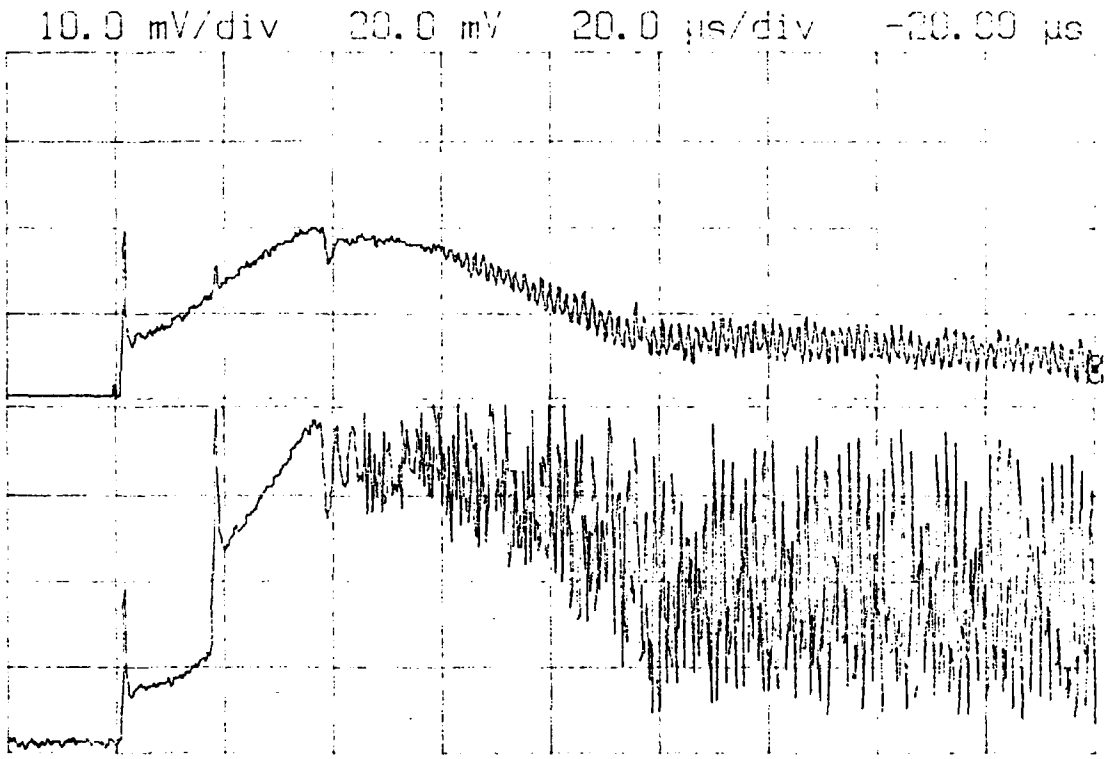

Figure 2.4.20 SF_6 pressure is between 4.3-5 Torr. Immediate partial response of the transmitted pulse, which responds again at 18-19µs.

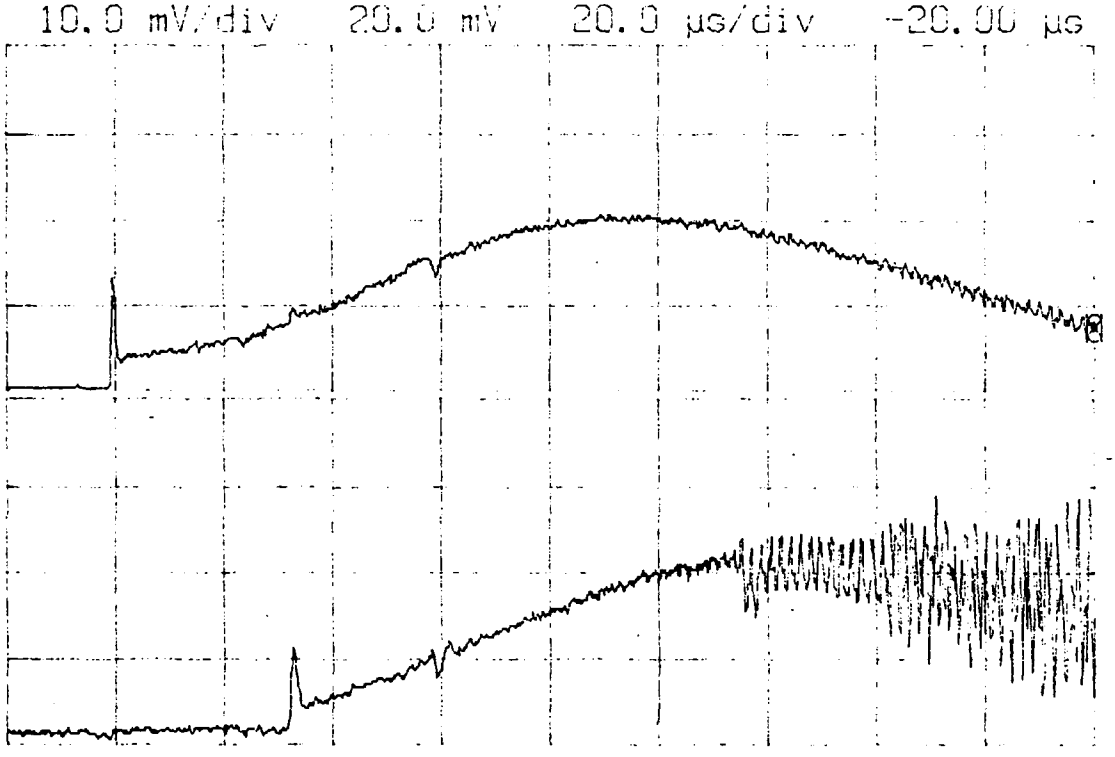

Figure 2.4.21 SF_6 pressure: 4.0 Torr. Over 30µs delay in response.

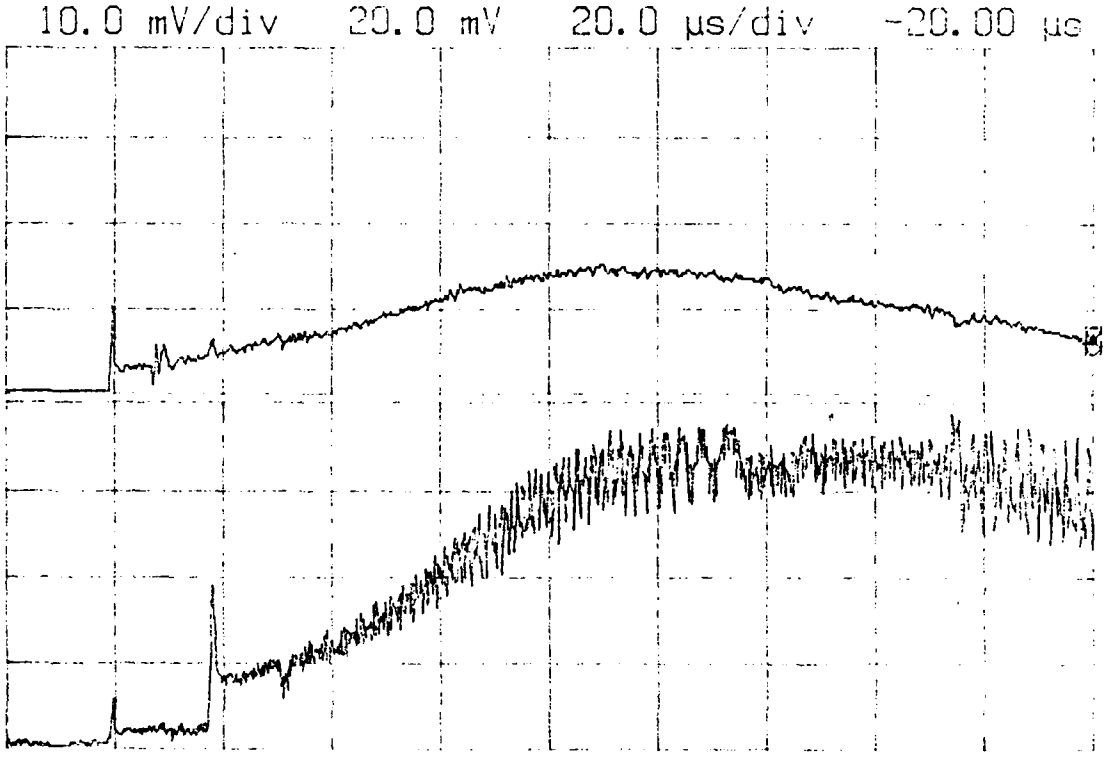

Figure 2.4.22 SF_6 pressure: 4.0 Torr. Partial fast response; secondary response at about 18µs.

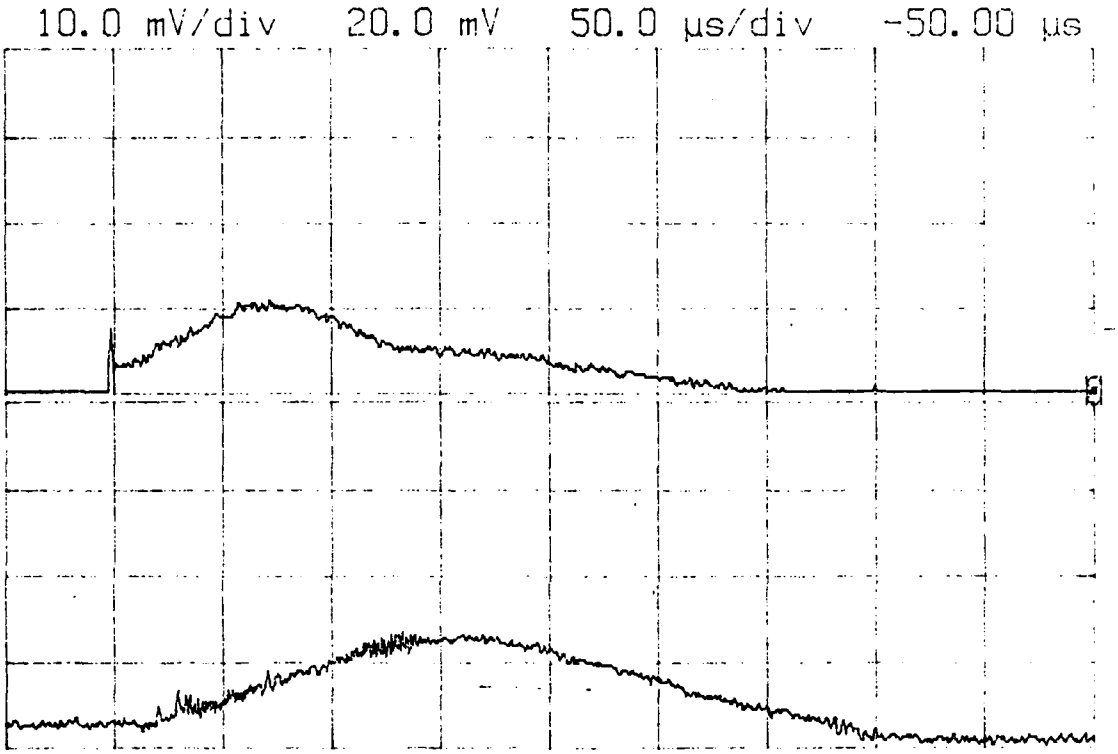

Figure 2.4.23 SF_6 pressure: 7.8 Torr. Delay and apparent suppression of the leading Q-switched pulse.

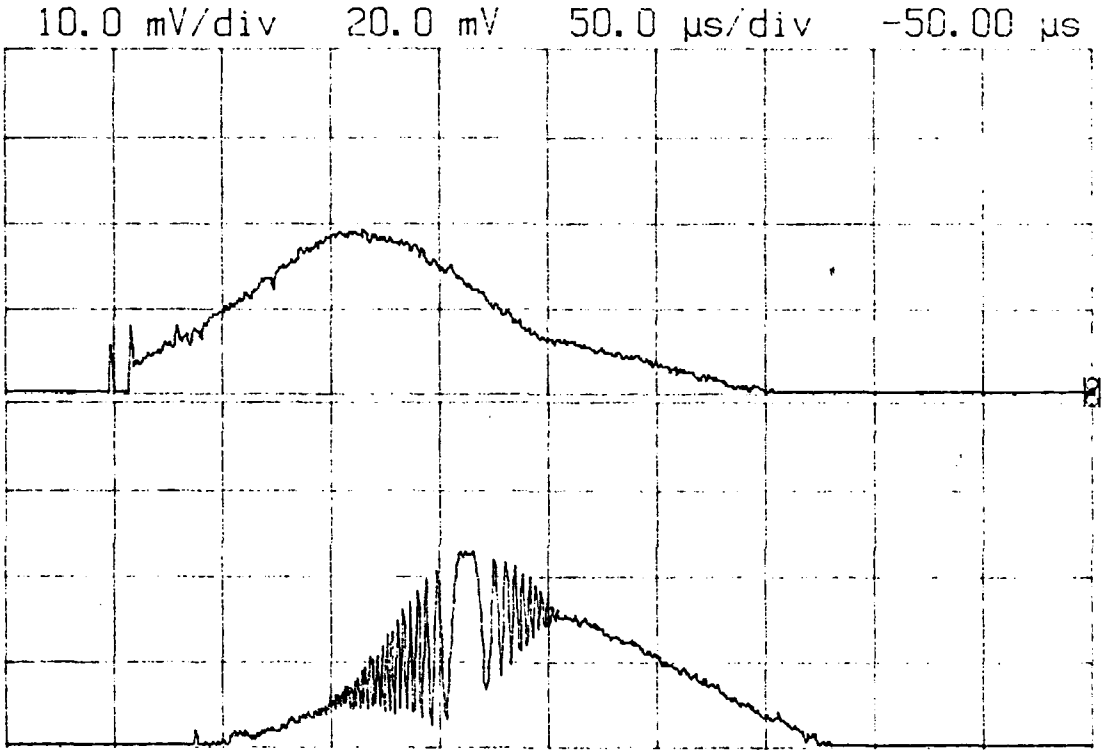

Figure 2.4.24 SF_6 pressure: 10.3 Torr. Similar to 2.4.23 in delay and Q-switched pulse suppression.

An experiment was run to determine whether or not the presence of 10.55μm radiation in SF_6 had an effect on the absorption of 16.26μm. Data was taken up to 4 Torr SF_6 pressure, again using the energy meter to detect the 16.26μm. No effect of 10.55μm on 16.26μm absorption was seen.

2.5 Task 5 - Design for scaled-up testing

Because of difficulties encountered in Task 4 in demonstrating the grating, we were not in a position to specify the nonlinear medium nor to begin design for scaled-up testing. Therefore no effort was expended on this task.

3.0 SUMMARY

Three potential candidates have been identified for the nonlinear medium to be used in beam combining by near-resonance nonlinear dispersion: 1,1,1 - trifluoroethane (H_3CCF_3) and methyl fluoride (CH_3F), which would interact with HF and CO_2 lasers, and sulfur hexafluoride (SF_6), which can interact with two CO_2 beams, or with a CO_2 beam and a 16.26μm beam from a CF_4 laser. Of these, SF_6 was selected, primarily because its properties are relatively well known. A computer program which evaluates dispersion relations for a three level system was modified to include dependence on a spatially varying incident radiation field. The necessary spectroscopic data and anharmonicity constants for SF_6 were input to the code and coupled with the spatial amplitude dependence of the incident 16.26μm (pump) field. The output was an index-of-refraction map as seen by the probe field. Examples of a single grating cycle as calculated by the code are shown in references 17 and 18, which are reproduced here as appendices, since that work is part of the contract effort.

The probe beam interaction with the grating has been modeled using coupled wave theory for each of the orthogonal incident linear polarizations, E-mode and H-mode. Gratings have been designed which will combine more than two beams. but the simplest possible system, a sinusoidal grating created by two pump beams for combining two probe beams, was chosen to demonstrate proof-of-principle. Computer codes were written for single probe beam diffraction by the grating, and for two beam combination by the grating. The latter programs allow for variations in the relative phases of the beams to be combined, and variation of the incident angle for either one of the incident beams. Diffraction and combination efficiencies are very sensitive to deviations from the Bragg angle, as expected for thick gratings. Combination efficiency varies only slowly with relative phase differences in the incident beams.

The analysis used so far for beam interactions is modeled on uniform amplitude plane waves of infinite extent. This simple model is excellent for understanding the physical effects occurring and for the initial work in grating design; clearly, an experimental system is less simple. Plane waves with gaussian amplitude profiles are more realistic. Saturation effects may also create nonsinusoidal gratings.

An experimental setup has been assembled for proof-of-principle demonstration. A CF_4 laser was built which can provide two beams of 16.26μm radiation of up to ~75μJ each at the interaction cell.

Experimental data were acquired for the transmission of 10.55μm pulses of ~100μs duration, ~100W peak power, through a 1.66cm thickness of pure SF_6. The measured absorption coefficient at pressures of 2 Torr or below gave reasonable agreement with previously published values. Above ~4 Torr SF_6 pressure, delays of the transmitted pulses of up to 30μs were observed, along with changes in pulse shape. At pressures near 8-10 Torr, suppression of a leading Q-switched pulse was also observed.

Measurements were made on the transmission of 16.26μm energy through a 1.81cm path in SF_6. Absorption coefficients in pure SF_6 appear to have reasonable values. Addition of helium as a buffer gas tends to suppress absorption of 16.26μm in SF_6. For helium partial pressures above 2-3 Torr, absorption of 16.26μm in SF_6 essentially disappears.

Attempts were made to demonstrate the presence of a grating in SF_6 created by 16.26μm beams. The diagnostic technique used was to seek the expected diffraction of a 10.55μm probe beam. The zero order was monitored for a decrease in power, and we sought to detect power diffracted into the first order. Experiments which were run with substantial partial pressures of helium buffer gas before the effect of helium was uncovered gave null results; no diffraction was observed.

Preliminary experiments run with pure unbuffered SF_6 also did not demonstrate a grating. An experiment was run to investigate the effect of the presence of 10.55μm on 16.26μm absorption; no effect was seen.

We have answered many questions but there are obviously some unanswered questions, as one would expect. At this point we do not feel that we have obtained any results that negate the ultimate potential of this approach but rather they are the usual problems one expects to encounter in a new area of science. The next section discusses our recommended approach to future efforts based on past progress and what we have learned.

4.0 RECOMMENDATIONS

Some interesting technical questions have emerged in the performance on this contract. They lead naturally to the suggestions made here.

The most surprising result of the work was the suppression of 16.26μm absorption in SF_6 by the addition of small amounts of helium buffer gas. The cause of this effect is not obvious. Possible explanations include shift of the Q-branch absorption edge away from the 16.26μm laser frequency, or a dramatic reduction of the effective lifetime of the absorbing energy level, each due to the addition of helium. The latter explanation seems unlikely; although addition of helium does speed up molecular energy level relaxation rates, the time scales are on the order of 10-100μs, while the 16.26μm pulse width will be in the order of the pumping CO_2 TEA pulse, which has a ~50ns FWHM.

Careful examination of 16.26μm absorption effects in SF_6 with fast detectors which can follow evolution of the pulses is in order. Measurements should be made in unbuffered SF_6 over a pressure range broad enough to determine if the effects seen with 10.55μm are observed with 16.26μm. Furthermore, since an original premise of this work was to operate in a collision-dominated regime, it is equally important to determine the effects of buffer gas addition. The effect of helium addition should be reexamined while using the fast detectors. We further recommend addition of argon and xenon as buffer gases to help sort out collisional effects; the molecular weight of argon (40) is ten times larger than He, while the weight of Xe (131) is close to that of SF_6 (146).

Another unanswered question is whether or not the interaction of 10.55μm radiation with SF_6 affects the absorption/interaction of 16.26μm. This knowledge is important in the long run as well as the short. The single experiment run to investigate this question did not have the fast 16μm detectors available, and therefore should be rerun carefully under various conditions of SF_6 pressure, 16.26μm beam intensity, 10.55μm beam intensity, absence or presence of buffer gas, and buffer gas species, as above.

The spatial and temporal purity of both the pump and probe fields are certain to be important factors in the successful performance of experiments

involved with gratings. Spatially, plane waves of finite extent and gaussian transverse profile are the best that can be expected. Although TEM_{oo} laser beams can be expanded to reduce transverse amplitude variation and approach uniform amplitude, the trade-off is lower intensity. Deviations from temporal purity, especially in the pump beams which create the grating, can be devastating. Longitudinal mode competition in the pump laser would produce a band of frequencies (and therefore wavelengths) in the pump beams which could conceivably wash out the grating. A spread of wavelengths in the probe beam would compromise the interpretation of diffraction efficiency , and could be expected to seriously affect the ability to combine beams. Therefore, for the production and identification of the grating, it is imperative to achieve the best possible single frequency TEM_{oo} modes for both pump and probe fields. Once the presence of a grating has been demonstrated, experiments can proceed to determine quantitatively what are the effects of deviation from optimum conditions.

Performance of the suggested tasks will help establish the degree of viability for the use of near-resonance nonlinear dispersion in SF_6 as a mechanism for beam combining. Should the interaction of 16.26μm and 10.55μm radiation fields in SF_6 not prove suitable for this application, near-resonance nonlinear dispersion is not ruled out, but its attractiveness would be diminished. Thus it would be important to distinguish between the basic phenomenon and the specific system used to investigate it, if this is possible.

Doing the recommended experimental tasks with the associated theoretical effort is certain to generate new scientific results, because this is uncharted territory.

5.0 REFERENCES

1. "Coherent laser addition using binary phase gratings," J.R. Leger, G.J. Swanson, and W.B. Veldkamp, Appl. Opt. 26, 4391 (1987).

2. "Laser-Controlled Optics Using Near-Resonance Nonlinear Dispersion in Gaseous Media," M. Rokni and A.M. Flusberg, IEEE J. Quantum Electron, QE-20, 1324 (1984).

3. "Bragg Reflection by a Gain Medium Optically Pumped in a Grating Geometry," A. Flusberg and M. Rokni, IEEE J. Quantum Electron. QE-22, 730 (1986).

4. The Omega codes were developed by M. Neviere and D. Maystre for the Air Force Weapons Laboratory, Kirtland AFB, New Mexico. They were provided to LTV by the courtesy of Ms. Rhonda Marshall, Rocketdyne Division, Rockwell International Corporation, resident at Kirtland.

5. "Analysis and Applicatons of Optical Diffraction by Gratings," T.K. Gaylord and M.G. Moharam, Proc. IEEE 73, 894 (1985).

6. "Analysis of multiwave diffraction of thick gratings," R. Magnusson and T.K. Gaylord, J. Opt. Soc. Am. 67, 1165 (1977).

7. "Calculation of arbitrary-order diffraction efficiencies of thick gratings with arbitrary grating shape," S.F. Su and T.K. Gaylord, J. Opt. Soc. Am. 65, 59 (1975).

8. "Rigorous coupled-wave analysis of planar-grating diffraction," M.G. Moharam and T.K. Gaylord, J. Optc. Soc. Am. 71, 811 (1981).

9. "Rigorous coupled-wave analysis of grating diffraction - E-mode polarization and losses," M.G. Moharam and T.K. Gaylord, J. Opt. Soc. Am. 73, 451 (1983).

10. "Analysis of the ν_4 (615 cm^{-1}) Region of the Fourier Transform and Diode Laser Spectra of SF_6," K.C. Kim, W.B. Person, D. Seitz, and B.J. Krohn, J. Mol. Spectrosc. 76, 322 (1979).

11. "High-energy optically pumped molecular lasers in the 13- and 16-μm regions," J.J. Tiee, T.A. Fischer, and C. Wittig, Rev. Sci. Instrum. 50, 958 (1979).

12. "Isotopically pumped isotopic CF_4 laser," R. Eckhardt, J. Telle, and L. Haynes, J. Opt. Soc. Am. 72, 40 (1982).

13. "Experimental and theoretical investigation of a pulsed laser utilizing the CF_4 molecule," V.Yu. Baranov, D.D. Malyuta, Uy.V. Petrushevich, A.N. Starostin, A.P. Strel'tsov, and S.V. Khomenko, Sov. J. Quantum Electron. 16, 1433 (1986).

14. "Passive Q-Switching of a CO_2 Laser," O.R. Wood and S.E. Schwarz, Appl. Phys. Lett. 11, 88 (1967).

15. "Self-Induced Transparency in Gases," C.K.N. Patel and R.E. Slusher, Phys. Rev. Lett. 19, 1019 (1967).

16. "Self-Induced Transparency," R.E. Slusher, in Progress in Optics XII, E. Wolf, ed. (North Holland, 1974) pp. 53-100.

17. "Beam combining in a gas via nonlinear, diffractive optics," J. S. Chivian, C. D. Cantrell, W. D. Cotten, and C. A. Glosson, presented at O-E LASE '88, Los Angeles, CA, January 1988; Proc. SPIE 874, (1988) (to be published).

18. "Laser Beam Combining Using Near-Resonance Nonlinear Dispersion," C. A. Glosson, C. D. Cantrell, J. S. Chivian, and W. D. Cotten, presented at the 1988 Conference on Lasers and Electro-Optics (CLEO '88), Anaheim, CA, April 1988.

APPENDIX A

Beam combining in a gas via nonlinear, diffractive optics

Jay S. Chivian*, C. D. Cantrell**, W. D. Cotten*, and C. A. Glosson**

*LTV Missiles and Electronics Group, Missiles Division
P. O. Box 650003, Dallas, Texas 75265

**University of Texas at Dallas, Center for Applied Optics
P. O. Box 830688, Richardson, Texas 75083

ABSTRACT

Near-resonance nonlinear dispersion is used to create a periodically modulated index of refraction in a collection of three level systems. This modulation causes the coherent combination of two incident probe beams into a single output beam.

1. INTRODUCTION

There has been recent interest in applications requiring lasers with intensities greater than those currently available. In order to achieve these ends, it is necessary to combine several laser beams coherently into the desired beam of increased intensity. A simple manner in which this can be achieved is to couple the beams in a diffraction grating. Veldkamp, Leger, and Swanson have recently optimized a grating pattern using an iterative computer program, then etched that pattern onto a thin quartz substrate, subsequently demonstrating the coherent addition of as many as seven incident beams.[1-3] Rockni and Flusberg discuss the possibility of using near-resonance nonlinear dispersion in a collisionally dominated gas for laser controlled optics including the creation of gratings.[4,5] This involves using one of the transitions in a three level system to modulate the index of refraction for radiation nearly resonant with the other transition in a non-reciprocal manner. The importance of this result is that it is possible for a few pump beams to control stronger probe beams in a gaseous medium. A nonpertubative method of calculating the complex index of refraction has been developed for just such a system of three level atoms or molecules by Adams, Cantrell, and Louisell.[6]

One must carefully distinguish the non-reciprocal interaction of two beams under collision-dominated conditions, as discussed here and in [4], from four-wave mixing. In particular, the Manley-Rowe relations do not apply to an open system such as we consider. The efficiency of our beam combining scheme depends on the losses experienced by both the pump and probe beams, as well as on weak effects of the probe on the pump.

We show that it is possible to use near-resonance nonlinear dispersion to combine two input probe beams. Choosing for our medium SF_6 since its properties are reasonably well known,[7] we create a grating to control radiation near 945 cm^{-1} with CF_4 laser radiation nearly resonant with the ν_4 mode of SF_6 at 615 cm^{-1}. The grating is designed such that all propagating orders have roughly equal intensities while all higher order waves are evanescent. We then solve the coupled equations (derived from the Helmholtz wave equation) necessary to find the transmission coefficients in a diffraction geometry.[8,9] The combining geometry is obtained from the diffraction geometry by reversing the direction of propagation for all of the probe waves, i.e. changing z into -z in the coupled wave equations.

Our method for beam combining utilizes a gaseous medium; thus the grating boundaries will be determined by the region of overlap between the pump laser beams which create the gratings, or by the walls of the cell containing the gas, as opposed to solid etched boundary. The grating will therefore consist of a spatial modulation of the complex index of refraction (or equivalently, the complex dielectric constant) of the medium. We treat the problem by considering low intensity plane waves propagating through an absorbing medium in a steady state that is independent of the intensities of the laser beams. This is the generalized coupled wave approach which allows for periodic index variations, and which also treats transverse electric (TE) or transverse magnetic (TM) polarization. It is summarized by Gaylord et. al.[8,9]

2. THEORY

A simple manner in which to approach this problem is to consider the diffraction of a single beam by a grating, then realize that one obtains the solution to the beam combination problem by changing z to -z in the resulting coupled equations. Given a single incident beam, we desire to produce a series of output beams with roughly equal

intensities while forcing all other output orders to be evanescent. Since we are working with a gaseous medium, we are necessarily in the thick grating regime. This complicates the analysis somewhat unless we consider a grating created by two pump beams.

We begin with the scalar Helmholtz equations for TE mode polarization and TM mode polarization, then expand the field variables in homogeneous plane waves using the vector Floquet condition. The dielectric constant is expanded in a complex Fourier series. These expansions are then substituted back into the Helmholtz equations producing the sets of coupled linear differential equations with constant coefficients: for the TE mode,

$$\frac{i}{2\pi^2}\frac{d^2S_j}{dz^2} - i\frac{2}{\pi}\left[\frac{(\varepsilon_o)^{1/2}\cos\theta}{\lambda} - \frac{j\cos\phi}{\Lambda}\right]\frac{dS_j}{dz} + \left[i\frac{(\varepsilon_o)^{1/2}\Lambda^2}{2\pi\lambda}\zeta + \frac{2j(m-j)}{\Lambda^2}\right]S_j +$$

$$+ \frac{2}{\lambda^2}\sum_{n=1}^{\infty}\left[S_{j-n}\,\varepsilon_n + S_{j+n}\,\varepsilon_{-n}\right] = 0 \qquad (1)$$

and for the TM mode,

$$\frac{i}{2\pi^2}\frac{d^2U_j}{dz^2} - i\frac{2}{\pi}\left[\frac{(\varepsilon_o)^{1/2}\cos\theta}{\lambda} - \frac{j\cos\phi}{\Lambda}\right]\frac{dU_j}{dz} + \left[i\frac{(\varepsilon_o)^{1/2}\Lambda^2}{2\pi\lambda}\zeta + \frac{2j(m-j)}{\Lambda^2}\right]U_j -$$

$$-\frac{i}{2\pi^2}\sum_{n-1}^{\infty}\left\{n\frac{2\pi}{\Lambda}\left(\frac{2\pi\varepsilon_n}{\varepsilon_o}U_{j-n}\left[\sin\phi\left(\frac{(\varepsilon_o)^{1/2}\sin\theta}{\lambda} - \frac{(j-n)\sin\phi}{\Lambda}\right) + \right.\right.\right.$$

$$\left.\left.\left. + \cos\phi\left(\frac{(\varepsilon_o)^{1/2}\cos\theta}{\lambda} - \frac{(j-n)\cos\phi}{\Lambda}\right)\right] -\right.$$

$$-2\pi\frac{\varepsilon_n}{\varepsilon_o}U_{j+n}\left[\sin\phi\left(\frac{(\varepsilon_o)^{1/2}\sin\theta}{\lambda} - \frac{(j+n)\sin\phi}{\Lambda}\right) + \right.$$

$$\left.\left. + \cos\phi\left(\frac{(\varepsilon_o)^{1/2}\cos\theta}{\lambda} - \frac{(j+n)\cos\phi}{\Lambda}\right)\right] +\right.$$

$$\left. + i\cos\phi\left(\frac{\varepsilon_n}{\varepsilon_o}\frac{dU_{j-n}}{dz} - \frac{\varepsilon_{-n}}{\varepsilon_o}\frac{dU_{j+n}}{dz}\right)\right] + k^2(\varepsilon_n U_{j-n} + \varepsilon_{-n}U_{j+n})\Bigg\} = 0 \qquad (2)$$

where θ is the angle of incidence, ϕ is the angle the grating vector makes with the inward pointing normal to the surface, λ is the wavelength of the incident radiation, ζ is the absorption, Λ is the grating period, ε_o is the unmodulated dielectric constant, and m is the Bragg number defined as

$$m = \frac{2\Lambda(\varepsilon_o)^{1/2}}{\lambda}\cos(\theta-\phi). \qquad (3)$$

An illustration of this system is shown in Figure 1. Any arbitrary polarization can then be written in terms of its TE and TM components.

If we were to consider gratings created by more than two pump beams, the equations that result from the coupled wave approach will have Fourier components for the modulation of the dielectric constant which depend on spatial position. The resulting equations will then have nonconstant coefficient equations. Since the analysis must be valid for the thick grating regime and since an eigenvector/eigenvalue solution seems to be the most expedient one for solving constant coefficient equations, we have chosen for purposes of this paper to exclude gratings formed by more than two pump beams. Furthermore, two pump beams can create only a sinusoidal modulation in the intensity regime of interest and sinusoidal grating profile can effectively couple only the 0 order and the +1 order beams for weakly modulated gratings. Hence, we consider also only two probe beams incident on the grating.

In order to calculate the effect of one laser beam on the index of refraction experienced by another we calculate the expectation value of the molecular dipole moment $\langle\mu\rangle$ at the laser frequency of interest, and then apply the dilute-medium approximation to calculate the induced dipole moment per unit volume as $P=N\langle\mu\rangle$ (where N is the number of molecules per unit volume). If P is expressed as $P=\chi E$ (where E is the amplitude of the

laser electric field) then the complex index of refraction, n, is $n=(1+4\pi\chi)^{1/2}$. We calculate $\langle\mu\rangle$ using a density matrix evaluated in the steady-state approximation, in which laser excitation is balanced by collisional damping. This approach has the advantage that it includes saturation effects to all orders in all laser fields present. It can be shown[4] that for collision dominated conditions, $|\beta_1| >> |\beta_2|$ in the equations for the nonlinear parts of the index of refraction

$$\Delta n^{NL}(\omega_2)=\beta_1|E_1|^2 \quad (4)$$

$$\Delta n^{NL}(\omega_1)=\beta_2|E_2|^2 \quad (5)$$

The implication of this relation for beam combining is quite clear. Strong fields nearly resonant with the $|1\rangle \rightarrow |2\rangle$ transition will have only a small effect on the nonlinear index of refraction for radiation at the $|0\rangle \rightarrow |1\rangle$ transition. Hence, weak fields can be used to establish a periodic modulation of the index of refraction for the $|1\rangle \rightarrow |2\rangle$ transition which acts to combine several strong laser fields into a single output field while these strong fields have only a slight effect on the weak fields.

The model we currently use for SF_6 is a simple, nondegenerate ladder with three energy levels corresponding to the ground vibrational state and the ν_4 and $\nu_3+\nu_4$ excited vibrational states. This model was chosen because it is simple to implement numerically and because it includes the essential phenomena of coherent driving, saturation, and collisional damping. However, the model is too simple to include multiphoton absorption, which is known to occur in SF_6 and all other polyatomic molecules subjected to nearly resonant infrared excitation. Our current model also does not include vibrational degeneracy or molecular rotation, which creates many vibration-rotation levels in place of a single vibrational level.

The design of a grating suitable for combining N beams of roughly equal intensity in a thick grating is a considerable challenge. We can get some idea as to the complexity of the problem by examining the reverse situation: a single beam passing through a diffraction grating producing many output beams. The number of emergent beams depends on the ratio of the grating period to the wavelength of the incident radiation. If the grating period is less than the incident wavelength, the incident beam will only be absorbed by the gas. As the grating period is increased beyond the wavelength of radiation, more than one output beam is allowed by the Bragg condition. Optimally, one would like to combine only as many beams as are allowed by the Bragg condition. In other words, all orders not used in the combining scheme must be evanescent. This restriction can be relaxed somewhat by allowing higher orders which are not evanescent but which carry negligible amounts of the energy.

More complexity exists when more than two pump beams create the grating. Specifically, for every pair of pump beams there exists one grating. For example, five pump beams will produce ten gratings. However, many of these gratings may contribute only to output noise if the proper grating profile is not carefully established. Also, as mentioned earlier, any number of pump beams greater than two will necessarily produce modulations in the direction of propagation. This renders solution of the equations by eigenvector-eigenvalue techniques ineffective since a new solution must be obtained at each z plane. With proper consideration, such complexity can be used to our advantage.

It is evident that grating design is not a simple process and is an integral part of the analysis, even in determining which method of solution is appropriate for the derived equations. Furthermore, the grating design must be technically feasible. At present, this means choosing simple grating profiles.

3. RESULTS

The energy-level diagram of a model of SF_6 is shown in Figure 2. The absorption coefficient for radiation at frequency 945 cm^{-1} is 0.4 cm^{-1} $Torr^{-1}$. Two beams of frequency 614.7 cm^{-1}, detuned by 0.3 cm^{-1}, incident on the gas cell at angles $\pm 30°$ with respect to the normal to the gas cell create a modulation of the index of refraction with period $\Lambda=16.26\mu m$. This is the system from which all calculations are made and is illustrated in Figure 1. The modulation profile, a single period of which is shown in Figure 3, serves to combine two probe beams with frequency 944.7 cm^{-1} incident at the 0 and +1 Bragg orders into the single desired output beam. Since the modulation of the imaginary part of the index of refraction is four orders of magnitude less than the modulation of the real part, it was neglected. Figures 4 and 5 show the resulting output beam as a function of the ratio of the thickness of the grating to the grating period, D/Λ, when the incident beams have a 0° and 180° relative phase difference, respectively. Notice that in Figure 5 the output direction is now that of the +1 order beam instead of the 0 order beam. This can be easily established by reference to the principle of linear superposition. Any beam can be considered to have a part in phase with other beam and a

part out of phase by $\pi/2$. The parts in phase coherently add in the gas while the parts our of phase pass through unaltered. We find that for phase difference satisfying $\Delta\phi<<\pi/2$ there is still good beam combination, for phase differences $\Delta\phi\approx\pi/2$ there is no interaction between the beams, and for phase differences $\Delta\phi\approx\pi$ the output order changes completely. We also find that the propagation distance for optimal combination can be altered significantly by changing the pump field strengths or the partial pressure of the active gas. Figure 6 shows the magnitude of the modulated index of refraction when either the field strengths of the pump beams are increased in the unsaturated gas or the partial pressure of SF_6 has been doubled. Figures 7 and 8 show the resulting output beams. The optimal propagation length now occurs at half the distance compared to the case depicted in Figures 4 and 5. Hence it is possible to tune the grating cell for maximum combination by altering the grating thickness or by altering the partial pressure of the active gas.

4. EXPERIMENT

A schematic of the experimental apparatus is shown in Figure 9. The illustration shown assumes that SF_6 is in the sample cell, but there are some general comments that can be made for arbitrary pump, probe, and sample combinations.

The beam splitter-detector combination immediately beyond the output mirror of each laser samples the output pulse of its related laser. Calibration of the beam splitter and detector in each case then gives a time sample of the laser power.

The mirror M_S in Figure 9 can be placed in one of the two positions shown so that the spectrum analyzer can sample either the probe beam, or the beam which is used to optically pump the pump laser. If it is desired to use the spectrum analyzer, the appropriate detector must be moved out of the relevant beam line.

The second of the beam splitters beyond the pump and probe lasers provides the amplitude separation of each beam which is needed so that two (or more) pump beams may create a grating in the sample cell, and two (or more) probe beams may be combined. Calibration of the beam splitter-mirror-sample cell window-detector trains are necessary in each case so that quantitative statements may be made about sample transmission. The angles of incidence for the pump and probe beams are chosen by predictions from theory. All calibrations are made after satisfactory alignment of the apparatus.

In the simplest case in which a grating is created by two pump beams, the grating spacing is determined by the angle between the pump beams. Any grating may be examined by a single probe beam by blocking all other probe beams. A probe beam angle may be changed by translating and rotating one or more mirrors as needed. The phase of one probe beam with respect to another may be varied by translating one mirror in a direction normal to its surface by fractions of a wavelength. In order to maintain coherence between any two beams, it is convenient to make their optical paths roughly the same. The additional necessity of keeping track of timing sequences also lends importance to equalizing optical paths. This will be especially true when a delay is introduced into probe pulse inception for the purposes of examining grating persistence and decay characteristics.

The detector (shown with integrating sphere) behind the sample cell looks at probe radiation transmitted through the sample. For a single probe beam, the detector can be moved to test for the presence or absence of various orders of diffracted radiation. In a combining experiment it will be convenient to have two or more detectors in appropriate locations.

The output of each detector is routed to a fast transient digitizer, the output of which in turn goes to the microcomputer acting as a data collection and processing station.

Several considerations must be taken into account in designing the sample cell. The "strength" of the grating depends on the amount of sample gas present and on the amplitude of the pump beams forming the grating. For a given combination of these factors, there will be an optimum thickness of the grating for diffracting one beam into N equal beams (and thus combining N beams into one). A task of experimental design is to arrive at a workable combination of all the variables: the gas pressure, the pump beam intensity, the cell thickness, and the beam diameter of the pump beams. The last must be large enough so that the effective thickness of the grating is determined by the separation of the cell windows, and not limited by the region of overlap of the pump beams. Thus it is clearly seen that theory and experiment will influence each other strongly.

Selection of sample cell windows is also important. The ideal windows would transmit all of the incident light of both pump and probe beams regardless of angle of incidence. This is obviously impossible for any material. An uncoated low index material seems the best compromise, since reflections will be minimized, and there will be no coatings to be

angle sensitive. Potassium bromide is such a material; it has a wide transmission range (0.25μm-40μm) and its index is roughly 1.6-1.45 over this range.

Grating thickness can be varied by changing the separation between windows, provided the sample cell is made with this feature designed in, or grating strength can be varied by changing the gas pressure or pump beams intensity.

5. SUMMARY

We have shown that it is possible to use near-resonance nonlinear dispersion in a collection of three level systems to create a periodic modulation of the index of refraction. The modulation, effectively a diffraction grating, serves to couple a desired number of input beams into a single output beam. We explicitly demonstrate this for combining two laser beams with output efficiencies as high as 90%, with most of that loss arising from absorption in the medium.

6. ACKNOWLEDGEMENTS

Supported by the Office of Naval Research with funding from SDIO/IST, by Cray Research Inc., The University of Texas System Center for High Performance Computing, and the Texas Advanced Technology Research Program.

7. REFERENCES

1. W. B. Veldkamp, J. R. Leger, and G. J. Swanson, "Coherent summation of laser beams using binary phase gratings," Opt. Lett. 11, 303-305 (1986).

2. J. R. Leger, G. J. Swanson, and W. B. Veldkamp, "Coherent beam addition of GaAlAs lasers by binary phase gratings," Appl. Phys. Lett. 48, 888-890 (1986).

3. J. R. Leger, G. J. Swanson, and W. B. Veldkamp, "Coherent laser addition using binary phase gratings," Appl. Opt. 26, 4391-4399 (1987).

4. M. Rokni and A. M. Flusberg, "Laser-controlled optics using near-resonance nonlinear dispersion in gaseous media," IEEE J. Quantum Electron. QE-20, 1324-1331 (1984).

5. A. M. Flusberg and M. Rokni, "Bragg reflection by a gain medium optically pumped in a grating geometry," IEEE J. Quantum Electron. QE-22, 730-738 (1986).

6. D. R. Adams, C. D. Cantrell, and W. H. Louisell, "Multilevel, multifrequency laser pulse propagation," Opt. Comm. 43, 292-296 (1982).

7. C. D. Cantrell, V. S. Letokhov, and A. A. Makarov, in Coherent Nonlinear Optics: Recent Advances (Springer, 1980), pp. 165-269.

8. T. K. Gaylord, and M. G. Moharam, "Analysis and applications of optical diffraction by gratings," Proc. IEEE 73, 894-937 (1985).

9. R. Magnusson and T. K. Gaylord, "Analysis of multiwave diffraction of thick gratings," J. Opt. Soc. Am. 67, 1165-1170 (1977).

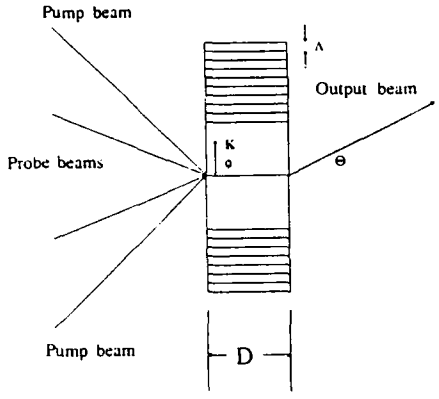

Figure 1. An illustration of the theoretical system used. The pump beams enter at angles $\pm 30°$, the probe beams enter at angles $\mp 18°$ (the 0 and +1 Bragg orders), the grating period is 16.26μm, and the output beam emerges at either the 0 or the +1 Bragg order.

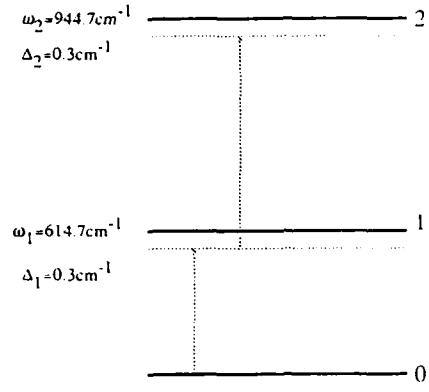

Figure 2. An illustration of the three level system for SF_6, where ω_i, i=1,2 is the laser frequency for the i-th beam and where Δ_i is the detuning of the i-th laser frequency from resonance.

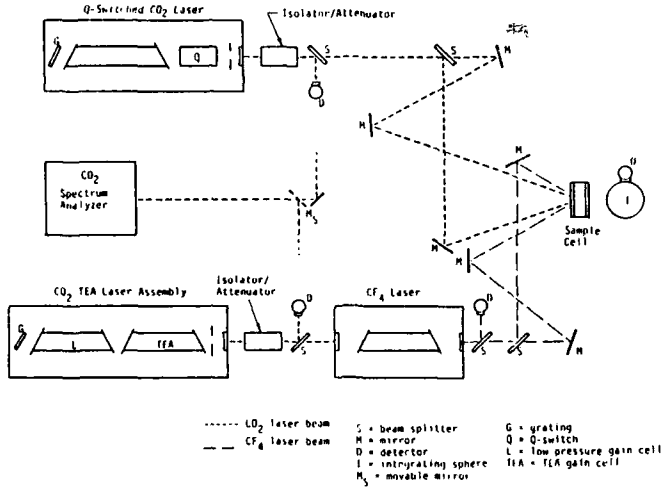

Figure 9. Schematic of beam combining experiments (not to scale).

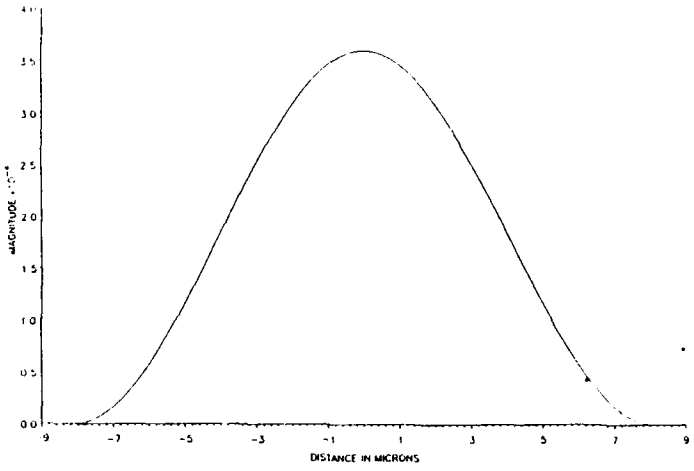

Figure 3. A singleperiod of the grating profile centered at the origin, created by two interfering plane waves of frequency 614.7 cm^{-1}, 0.1 Torr partial pressure of SF_6, and $|E_1| = 1.0$ sV cm^{-1}.

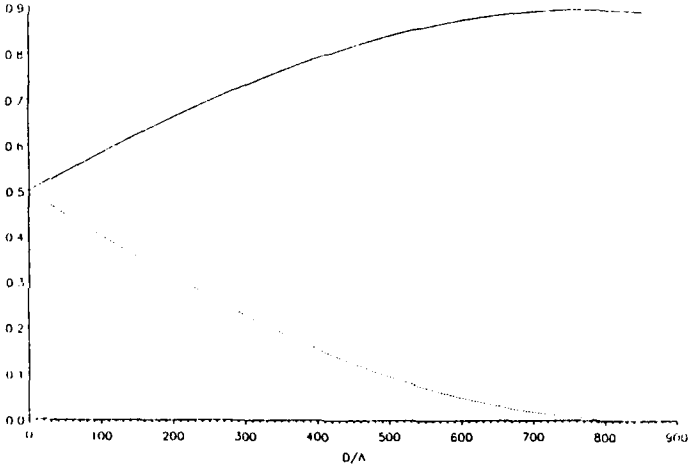

Figure 4. The diffraction efficiency for probe fields of frequency 944.7 cm^{-1} from the grating shown in Figure 3. The solid curve is the 0 output order and the dashed curve is the +1 output order. The input beams have a 0° relative phase difference.

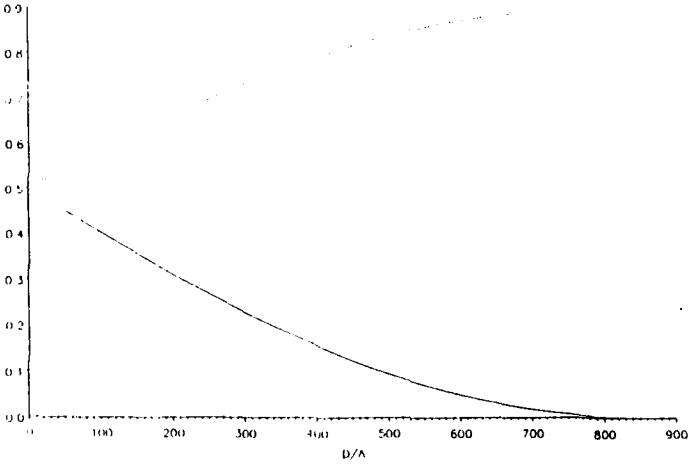

Figure 5. The diffraction efficiency for input beams having a 180° relative phase difference from the grating shown in Figure 3.

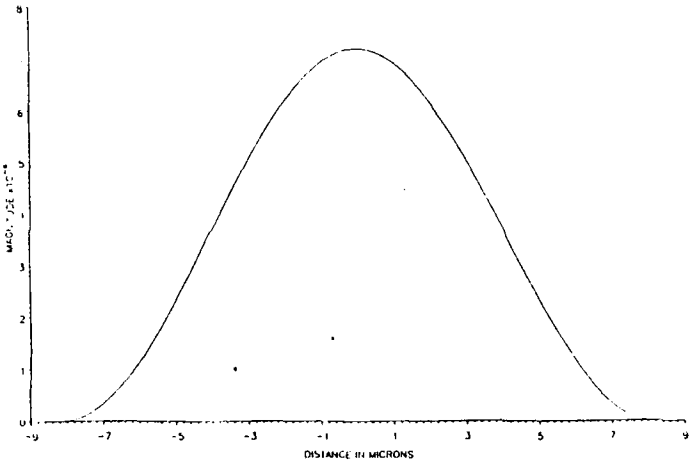

Figure 6. Similar to Figure 3 except with modulation twice as strong. This increase in modulation could arise from either an increase in the pump field strength if the strength is below the saturation threshold, or from a doubling of the partial pressure of SF_6.

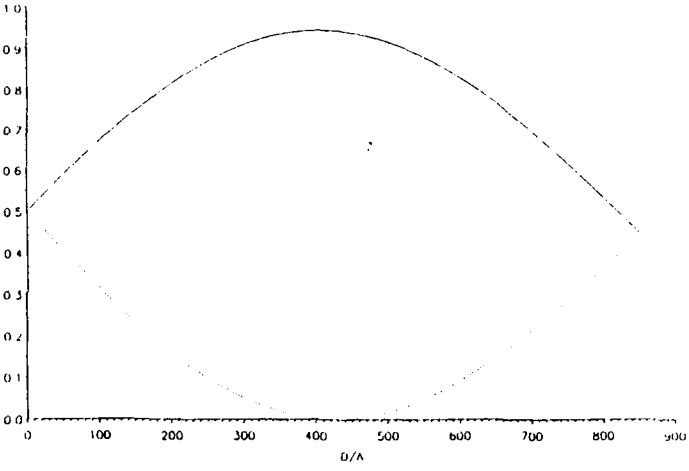

Figure 7. The diffraction efficiency for probe fields of frequency 944.7 cm^{-1} from the grating shown in Figure 6. The solid curve is the 0 output order and the dashed curve is the +1 output order. The input beams have a 0° relative phase difference.

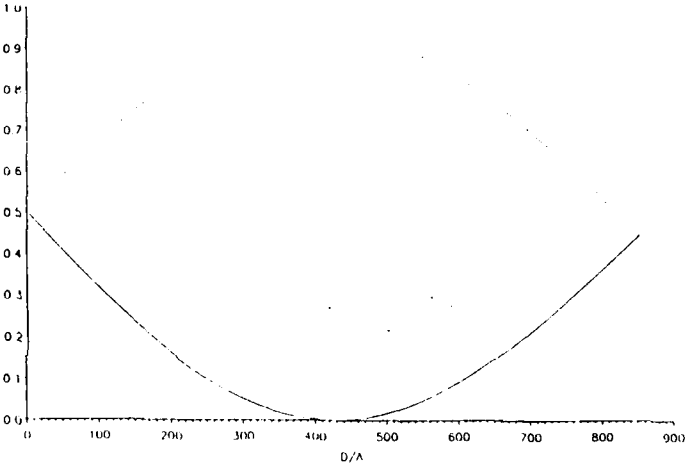

Figure 8. The difference efficiency for input beams having a 180° relative phase difference from the grating shown in Figure 6.

APPENDIX B

Laser Beam Combining Using Near-Resonance Nonlinear Dispersion*

C. A. Glosson**, C. D. Cantrell**, Jay S. Chivian† and W. D. Cotten†

**Center for Applied Optics
The University of Texas at Dallas
†LTV Missiles and Electronics Group

ABSTRACT

Near-resonance nonlinear dispersion is used to create a periodically modulated index of refraction in a collection of three level systems, acting as a grating for beam addition.

*Supported by the Office of Naval Research with funding from SDIO/IST

Laser Beam Combining Using Near-Resonance Nonlinear Dispersion*

C. A. Glosson**, C. D. Cantrell**, Jay S. Chivian† and W. D. Cotten†

**Center for Applied Optics
The University of Texas at Dallas
†LTV Missiles and Electronics Group

There has been recent interest in optics applications where lasers with intensities greater than those currently available are necessary. In order to achieve these ends, it is necessary to coherently combine several laser beams into the desired beam of increased intensity. A simple manner in which this can be achieved is via coupling in a diffraction grating. Veldkamp, Leger, and Swanson have recently optimized a grating pattern using an iterative computer program, then etched that pattern onto a thin quartz substrate, subsequently demonstrating coherent addition of as many as seven incident beams [1]. Rockni and Flusberg discuss the possibility of using near-resonance nonlinear dispersion in a collisionally dominated gas for laser controlled optics including the creation of gratings [2]. This involves using one of the transitions in a three level system to modulate the index of refraction for radiation nearly resonant with the other transition in a non-reciprocal manner. The importance of this result is that it is possible for a few pump beams to control several stronger probe beams in a gaseous medium. A nonperturbative method of calculating the complex index of refraction has been developed for just such a system of three level atoms or molecules by Adams, Cantrell, and Louisell [3].

One must carefully distinguish the non-reciprocal interaction of two beams under collision dominated conditions, as discussed here and in [2], from four-wave mixing. In particular, the Manley-Rowe relations do not apply to an open

*Supported by the Office of Naval Research with funding from SDIO/IST

system such as we consider. The efficiency of our beam-combining scheme depends on the losses experienced by both the pump and probe beams, as well as on weak effects of the probe on the pump.

We show that it is possible to use near-resonance nonlinear dispersion to combine two input probe beams. Choosing for our medium SF_6 since its properties are reasonably well known [4], we create a grating to control radiation near 950 cm^{-1} with CF_4 laser radiation nearly resonant with the ν_4 mode of SF_6 at 615 cm^{-1}. The grating is designed such that all propagating orders have roughly equal intensities while all higher order waves are evanescent. We then solve the coupled equations (derived from the Helmholtz wave equation) necessary to find the transmission coefficients in a diffraction geometry [5]. The combining geometry shown in Figure 1 is obtained from the diffraction geometry by reversing the direction of propagation for all of the probe waves, i.e. changing z into -z in the coupled wave equations. Figure 2 shows the results of combination in a lossy medium.

[1] W.B. Veldkamp, J.R. Leger, and G.J. Swanson, "Coherent summation of laser beams using binary phase gratings", Optics Letters **11**, 303-305 (1986).

[2] M. Rokni and A.M. Flusberg, "Laser-controlled optics using near-resonance nonlinear dispersion in gaseous media", IEEE Journal of Quantum Electronics **QE**–20, 1324-1331 (1984).

[3] D.R. Adams, C.D. Cantrell, and W.H. Louisell, "Multilevel, multifrequency laser pulse propagation". Optics Communications **43**, 292-296 (1982).

[4] C.D. Cantrell, V.S. Letokhov, and A.A. Makharov, in Coherent Nonlinear Optics: Recent Advances (Springer, 1980), pp. 165-269.

[5] T. K Gaylord, and M. G. Moharam, "Analysis and application of optical diffraction by gratings", Proc. IEEE 73, 894-937 (1985).

Figure Captions

Figure 1 Geometry of a grating induced by two pump beams and the resulting combination of two incident probe beams into one output beam.

Figure 2 This graph displays the transfer of energy from the +1 order beam (dashed line) to the 0 order beam (solid line) for zero phase difference as a fraction of the total incident intensity. The results shown are for a medium of SF_6 at a partial pressure of 0.1 torr, λ=10.55μm, and grating period Λ=16.26μm.

Beam Combining Geometry

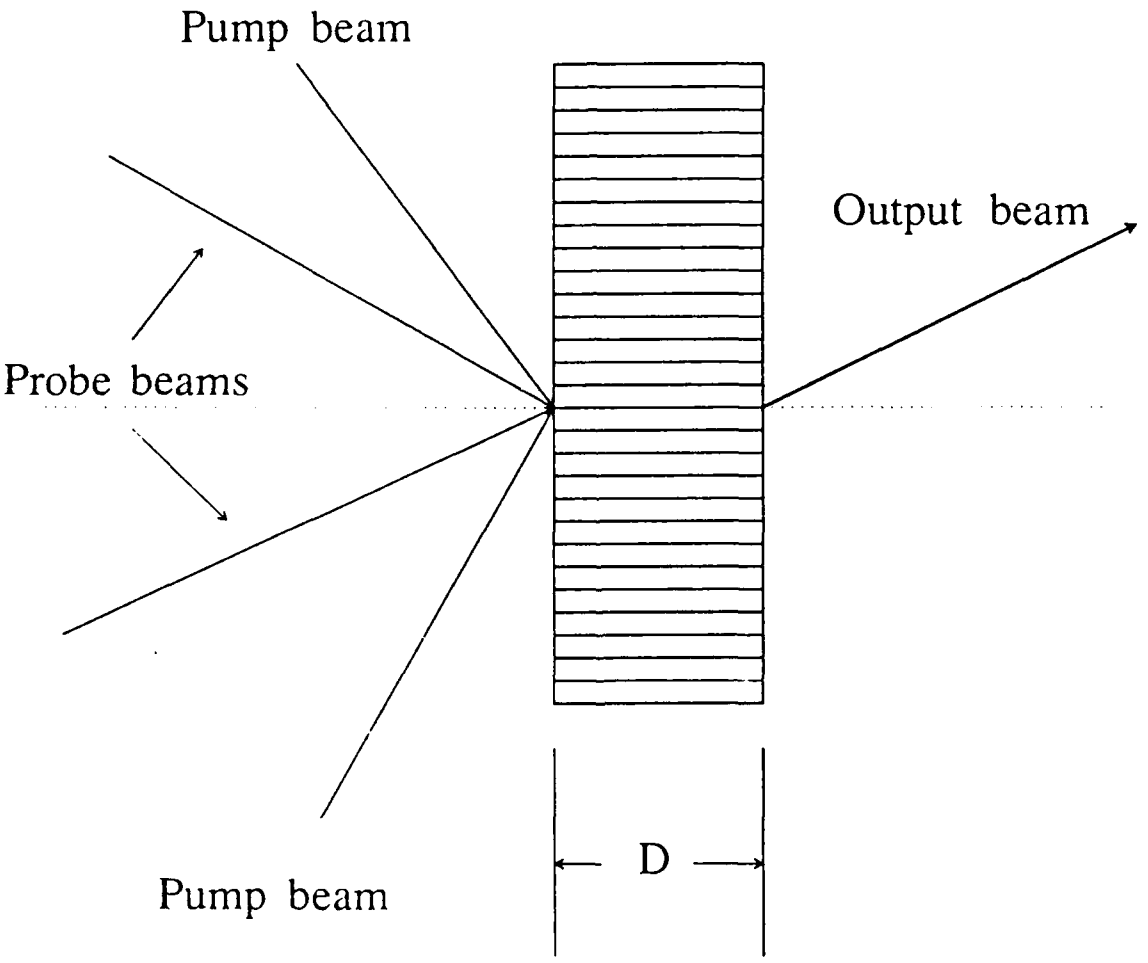

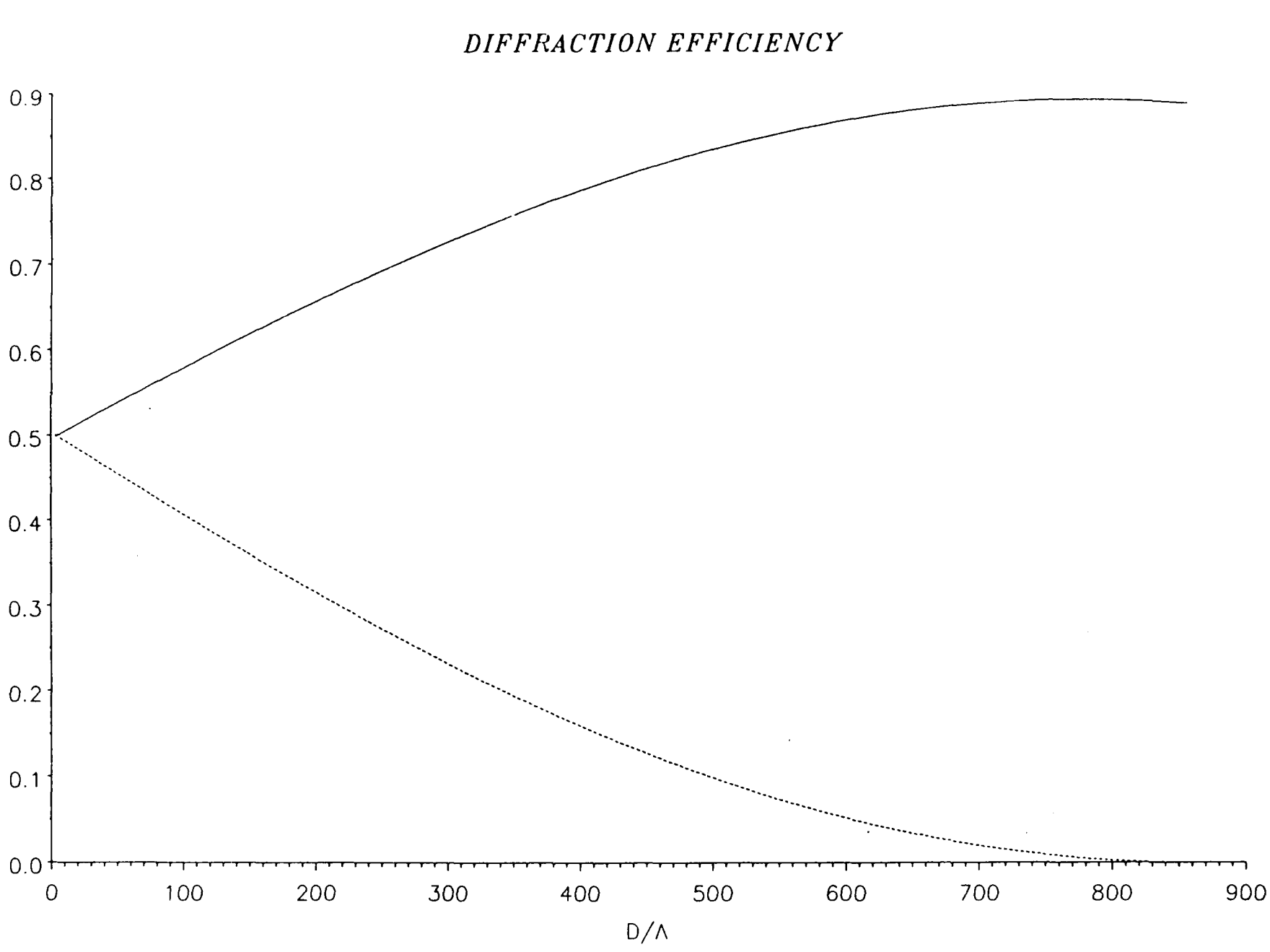
DIFFRACTION EFFICIENCY
0.9
0.8
0.7
0.6
0.5
0.4
0.3
0.2
0.1
0.0
0
100
200
300
400
500
600
700
800
900
D/Λ

LTV Missiles and Electronics Group
Missiles Division

UTD
The University of Texas at Dallas

Laser Beam Combining Using Near-resonance Nonlinear Dispersion†

C. A. Glosson*, C. D. Cantrell*, Jay S. Chivian**, and W. D. Cotten**

* University of Texas at Dallas, Center for Applied Optics

** LTV Missiles and Electronics Group, Missiles Division

† Supported by:

- Office of Naval Research with funding from SDIO/IST
- Cray Research Inc.
- The University of Texas System Center for High Performance Computing
- Texas Advanced Technology Research Program

Laser Beam Combining Using Near-resonance Nonlinear Dispersion

Near-resonance nonlinear dispersion is used to create a periodically modulated index of refraction in a collection of three level systems, acting as a grating for coherent beam addition.

What Features must the Combining System Have

- Combine N beams of roughly equal strength into a single output beam
- Maximum output efficiency
- Minimum beam loss
- Simple but effective system
    - System which is technically feasible
    - System which allows a thorough examination of the basic principles involved

Beam Combining with a Grating

- A properly shaped phase grating can combine N beams
  [J. R. Leger, G. J. Swanson, and W. B. Veldcamp
  Appl. Opt. 26 , 4391-4399 (15 Oct. 1987)]

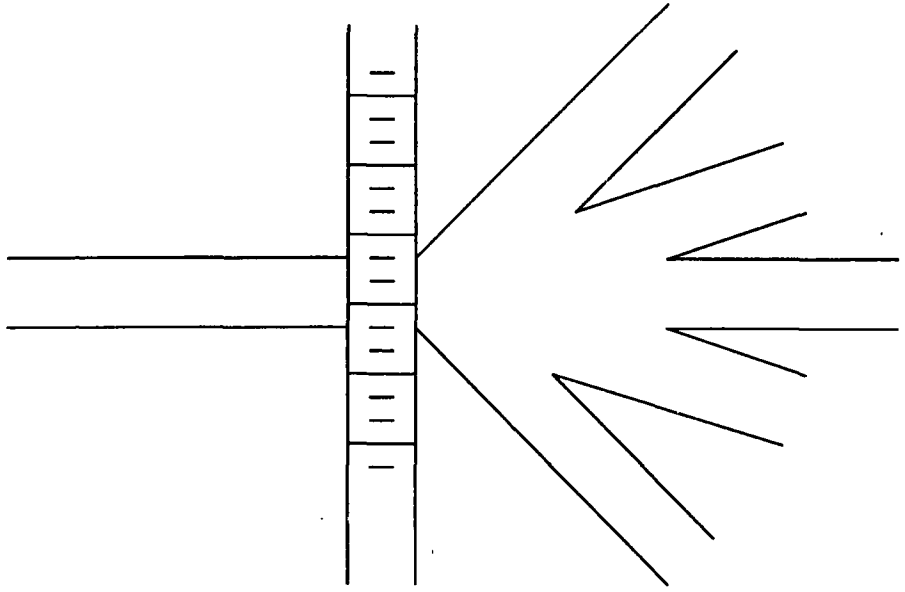

Conditions for Beam Combining with a Grating

- Phase-only (index) grating desirable to minimize losses
- Given the grating, radiation to be combined must have correct:
    - wavelength
    - polarization
    - amplitude
    - direction
    - phase relationship (coherence)
- Typically, design grating to produce N orders of equal amplitude

Creation of and interaction with the grating

- Near-resonance nonlinear dispersion involves two fields of different wavelengths interacting with the medium.

- Convenient to consider

  (a) creation of the grating

  (b) interaction with the grating

    - coupled wave approach

  [T. K. Gaylord and M. G. Moharam
  Proc. IEEE 73 , 894-937 (1985)]

Near-Resonance Nonlinear Dispersion

- Use nearly resonant excitation of a multilevel atom or molecule to create a grating with one beam that can interact with more powerful beams at another frequency.
  [M. Rokni, and A. Flusberg
  IEEE J. Quant. Electron. **QE-20** , 1324-1331 (1984)]

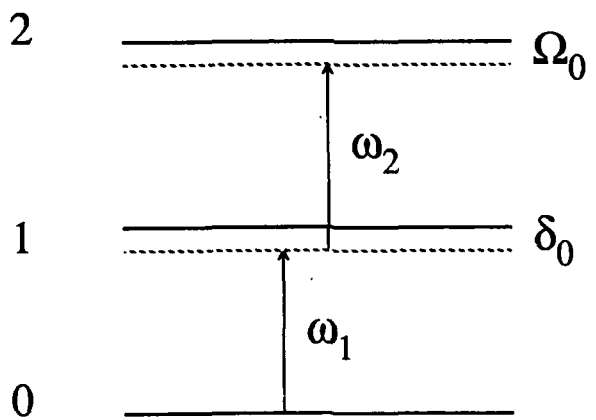

Application of Near-Resonance Nonlinear Dispersion

Basic idea: Under collision-dominated conditions, the change of the indices of refraction experienced by beams 1 and 2 are

$$\Delta n^{NL}(\omega_2) = \beta_1 |E_1|^2$$

$$\Delta n^{NL}(\omega_1) = \beta_2 |E_2|^2$$

where

$$|\beta_1| >> |\beta_2|$$

Application: Controlling the phase front of a laser beam at ω_2 using another, possibly much weaker, laser beam at ω_1.

Sulfur hexafluoride (SF_6)

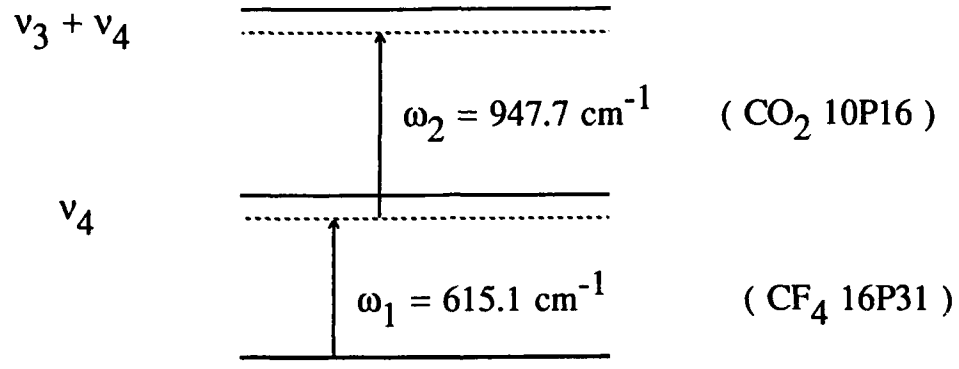

Calculation of complex index using a nonperturbative method of fields interacting with multilevel system.
[D. R. Adams, C. D. Cantrell, and W. H. Louisell
Opt. Comm. 43 , 292-296 (1982)]

Coupled Wave Approach

- Start with Maxwell's equations
- Leads to wave equations
- Assume harmonic waves $\mathbf{E}(\mathbf{r},t) = \mathbf{E}(\mathbf{r})\, e^{i\omega t}$
- Leads to the Helmholtz equations
- Assume a complex dielectric constant $\varepsilon = \Sigma\, \varepsilon_n e^{in\omega t}$
- Make the Paraxial approximation

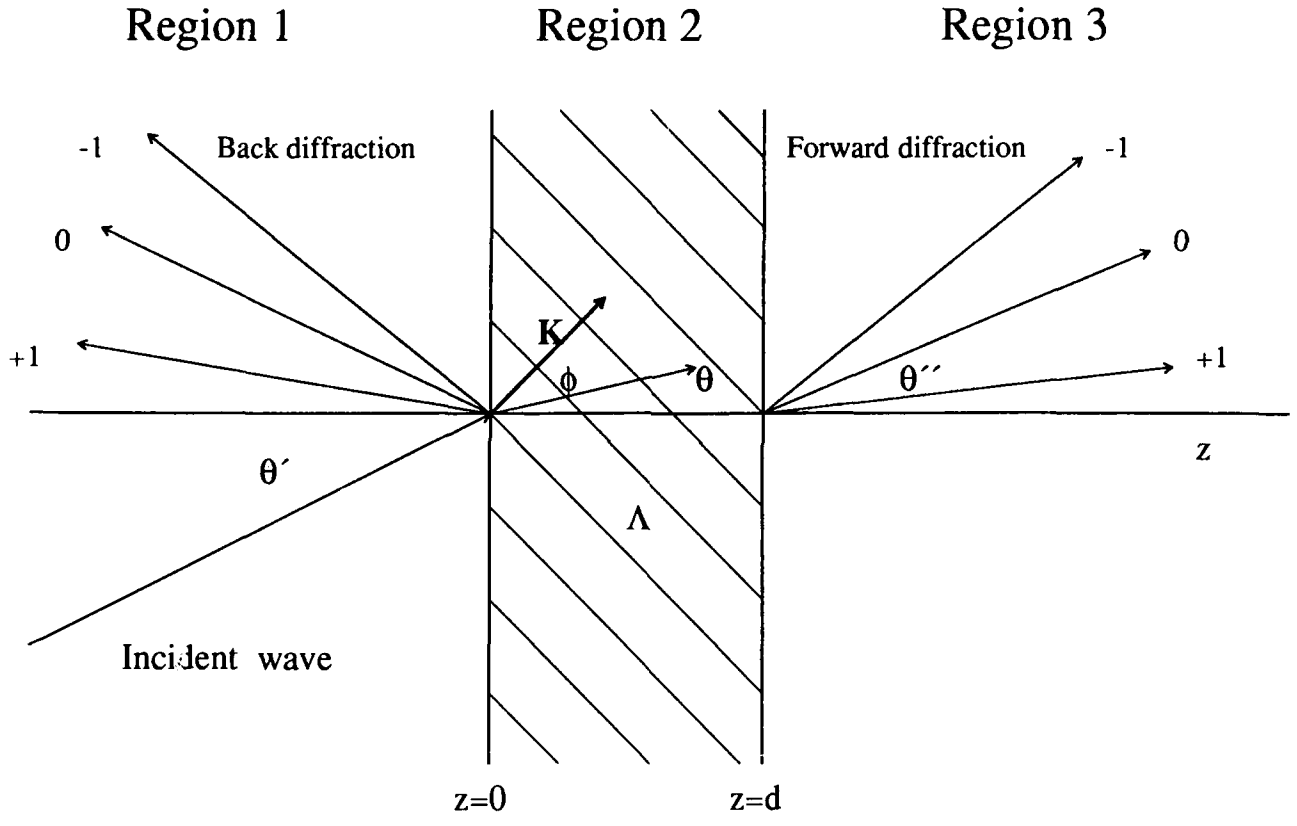
Region 1
Region 2
Region 3
-1
Back diffraction
0
+1
Forward diffraction
-1
0
+1
K
ϕ
θ
θ´´
θ´
Λ
z
Incident wave
z=0
z=d

TE mode ≡ H-mode

- $\nabla^2 E + k^2 \varepsilon E = 0$
- assume solution $E(x,z) = \Sigma S_j(z)\, e^{-i\sigma_j \cdot r}$

  where $\sigma_j = \sigma_0 - j\mathbf{K}$ is the vector Floquet condition
- $S_j = S_j(z)$ are inhomogeneous plane waves
  - amplitude varies across the phase front
- Substitute, do algebra

$$\frac{1}{2\pi^2}\frac{d^2 S_j}{dz^2} - \frac{i2}{\pi}\left[\frac{(\varepsilon_0)^{1/2}\cos(\theta)}{\lambda} - \frac{j\cos(\phi)}{\Lambda}\right]\frac{dS_j}{dz} + \frac{2j(m-j)}{\Lambda^2} S_j +$$

$$\frac{2}{\lambda}\sum_{n=1}^{\infty}\left[S_{j-n}\varepsilon_n + S_{j+n}\varepsilon_{-n}\right] = 0$$

Coupled wave equations with constant coefficients

where $\cos(\theta-\phi) = m\lambda / (2\Lambda(\varepsilon_0)^{1/2})$ defines m;

is the Bragg condition when m = integer

TE mode (cont)

- Rewrite $\frac{d^2S_j}{dz^2} = c_j \frac{dS_j}{dz} + b_j S_j + \sum_{n=1}^{\infty} \left[a_n S_{j-n} + a_n^* S_{j+n} \right]$

- Solve for $S_j(z)$

- In region 1: $E_1 = e^{-i\mathbf{k}_1 \cdot \mathbf{r}} + \sum R_j e^{-i\mathbf{k}_{1j} \cdot \mathbf{r}}$ (normalized)

- In region 3: $E_3 = \sum T_j e^{-i\mathbf{k}_{3j} \cdot (\mathbf{r} - \mathbf{dz})}$ R_j, T_j normalized

- By phase matching $\mathbf{k}_{1j} \cdot \mathbf{x} = \sigma_j \cdot \mathbf{x} = \mathbf{k}_{3j} \cdot \mathbf{x}$

$$(\varepsilon_1)^{1/2} \sin(\theta_j') = (\varepsilon_0)^{1/2} \sin(\theta) - j \left(\lambda / \Lambda \right) \sin(\phi)$$

$$(\varepsilon_3)^{1/2} \sin(\theta_j'') = (\varepsilon_0)^{1/2} \sin(\theta) - j \left(\lambda / \Lambda \right) \sin(\phi)$$

- Propagating or evanescent?

TE mode (cont)

- Transmitted orders $T_j = S_j(d)\, e^{-i(\sigma_0 \cos\theta - j\, K \cos\phi)d}$

- Reflected orders $\delta_{j0} + R_j = S_j(0)$

- Components of H related to E through Maxwell's equations

- Diffraction efficiency - transmitted wave

$$Re\left[\frac{\left[\left[\frac{\varepsilon_3}{\varepsilon_1} - \left(\sin\theta' - j\lambda \sin\phi / (\varepsilon_1)^{1/2}\Lambda\right)^2\right]\right]^{1/2}}{\cos\theta'}\right] T_j T_j^*$$

TM mode ≡ E - mode

- $\nabla^2 H - \left(\frac{\nabla\varepsilon}{\varepsilon} \bullet \nabla\right) H + k^2 \varepsilon H = 0$
- assume solution $H(x,z) = \sum U_j(z)\, e^{-i\sigma \bullet r}$
- $$\frac{d^2 U_j}{dz^2} = c_j \frac{dU_j}{dz} + b_j U_j + \sum_{n=1}^{\infty} \left[a_{j,n} U_{j-n} + a_{j,-n}{}^{*} U_{j+n} \right] + \sum_{n=1}^{\infty} \left[g_n \frac{dU_{j-n}}{dz} + g_{-n} \frac{dU_{j+n}}{dz} \right]$$
- Follow same procedure

A Simple Approach to Grating Design

- Conditions
  - All nonpropagating orders must be evanescent
  - Propagation occurs in the thick-grating regime
  - 2 pump beams ---> 1 grating
- Considerations
  - There exists a linear relationship between the number of propagating incident beams and the grating period
  - The Coupled-wave approach allows us to determine where the energy from the incident beams is transferred and how quickly this transfer occurs

Combining Two Beams

Why Two Beams?

- The simplest system with which to demonstrate the principle
- Requires only a one-dimensional grating
- Proper choice of incident angles will allow for a diffraction efficiency of 100% minus absorption losses

System for Beam Combination

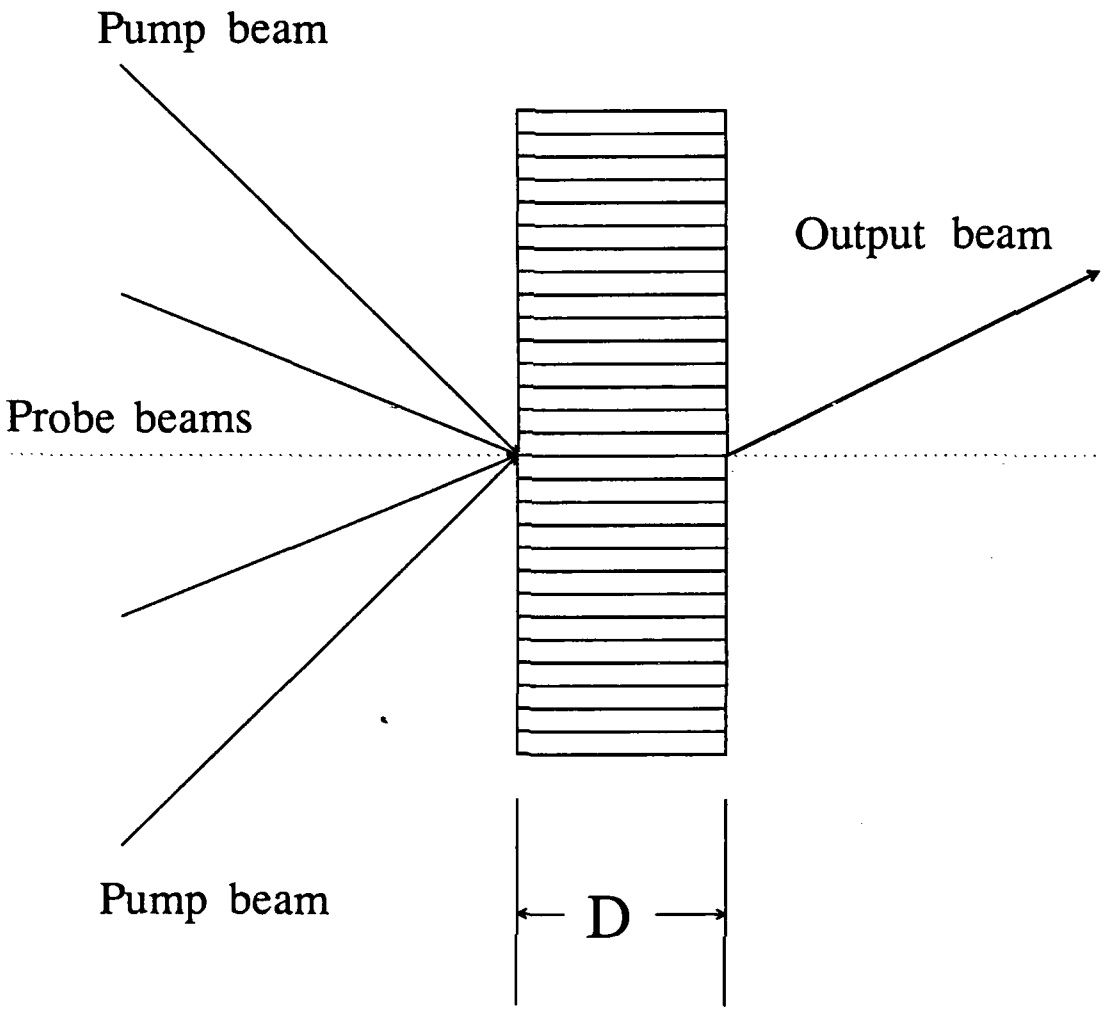

SINGLE GRATING CYCLE

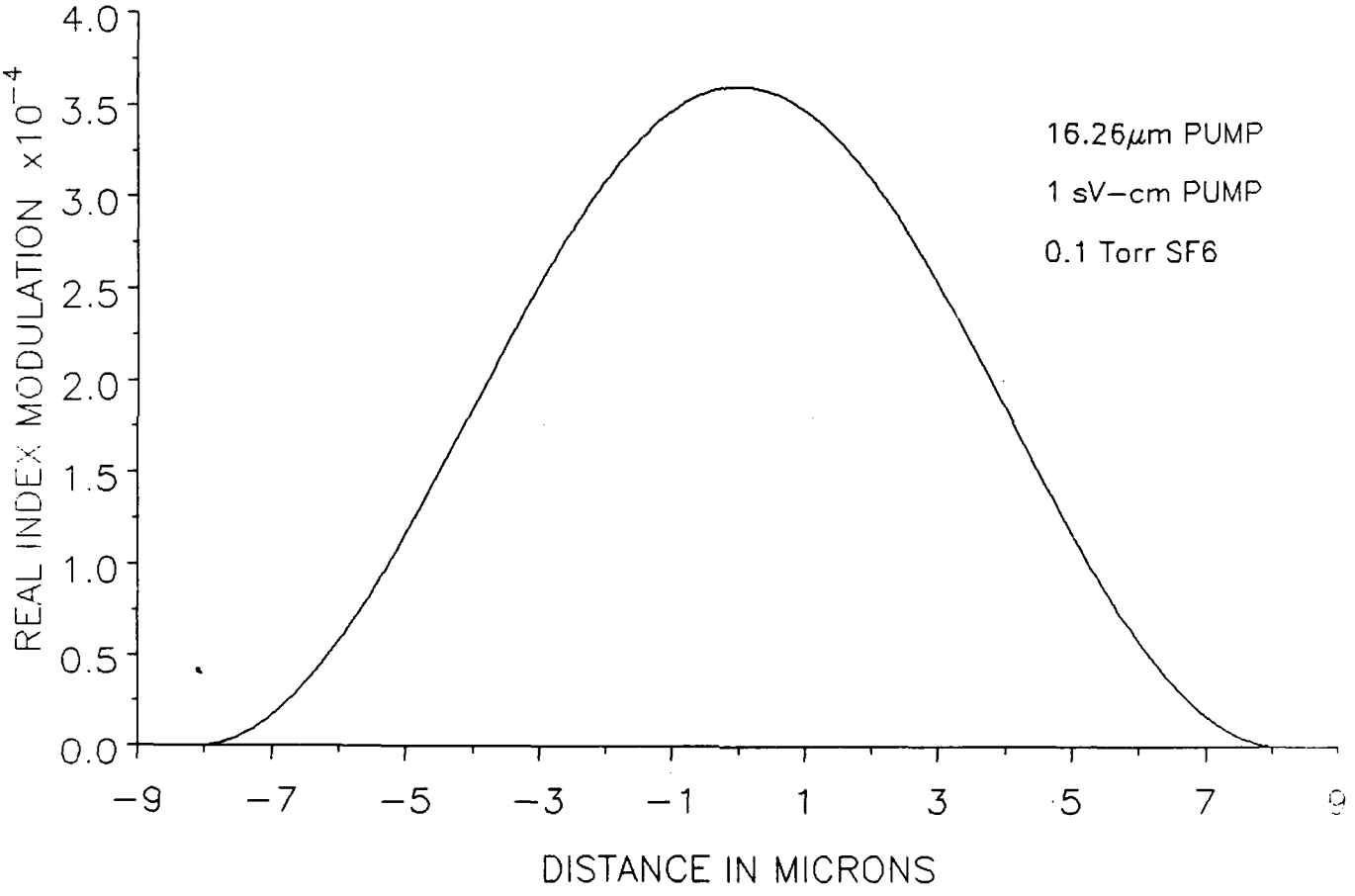

SINGLE BEAM DIFFRACTION

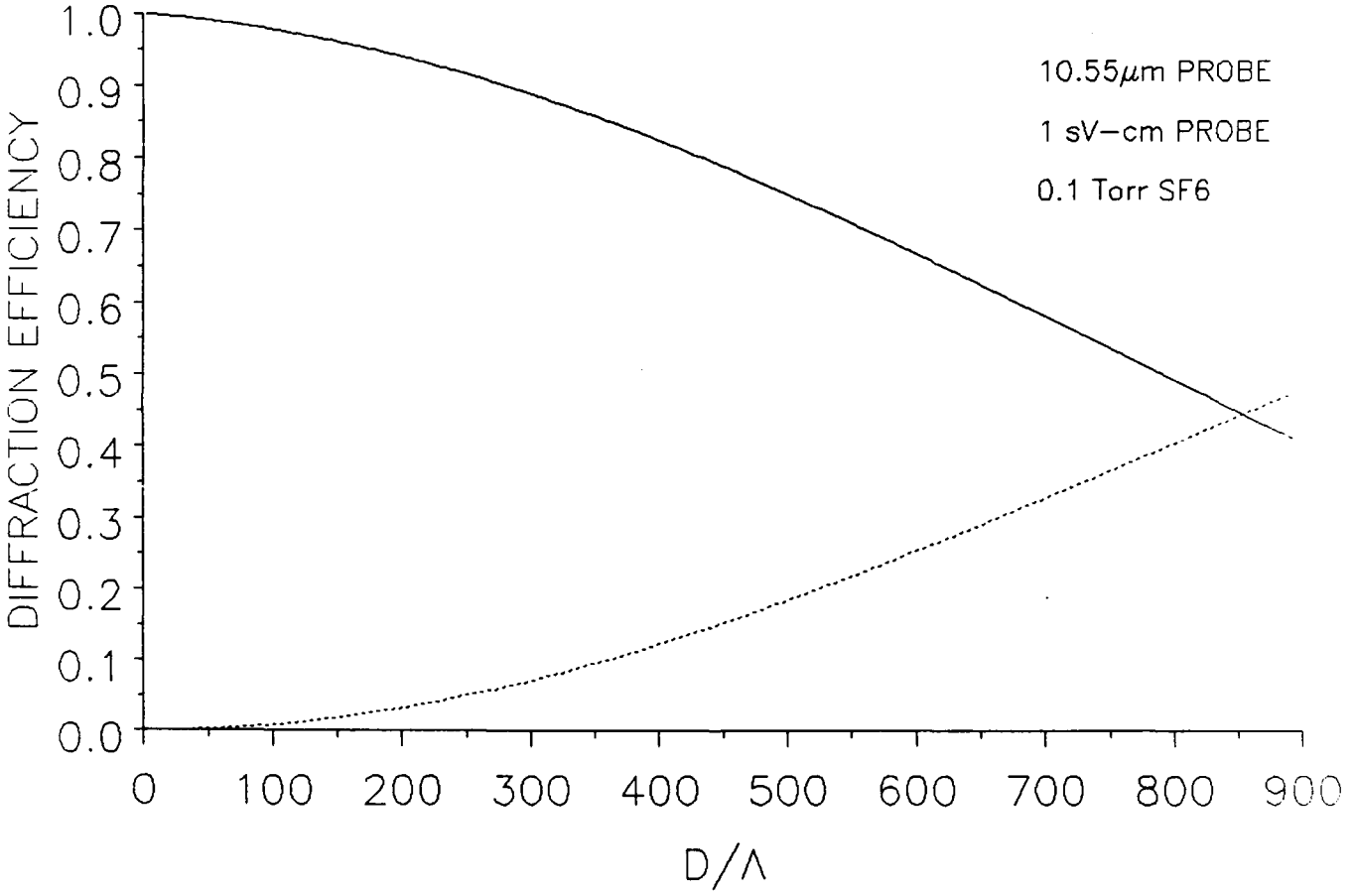

TWO BEAM COMBINATION EFFICIENCY

0 deg. RELATIVE PHASE DIFFERENCE

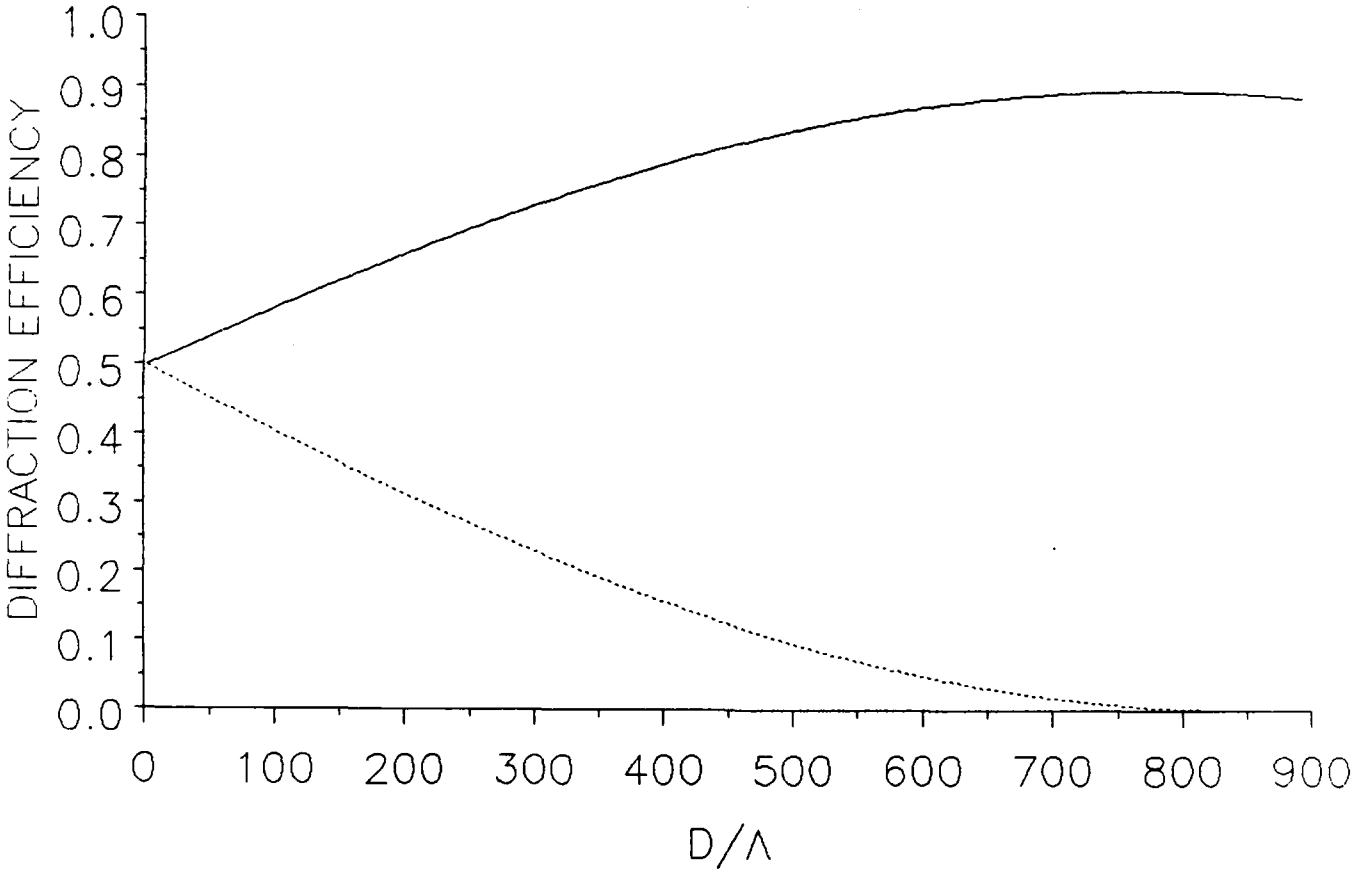

TWO BEAM COMBINATION EFFICIENCY

180 deg. RELATIVE PHASE DIFFERENCE